Available online at www.sciencedirect.com
ScienceDirect
PHYTOCHEMISTRY
Phytochemistry 68 (2007) 2351–2374
www.elsevier.com/locate/phytochem

Review

Experimental and mathematical approaches to modeling plant metabolic networks

Rigoberto Rios-Estepa [a,b], Bernd Markus Lange [a,*]

[a] *Institute of Biological Chemistry, M.J. Murdock Metabolomics Laboratory, Center for Integrated Biotechnology, Washington State University, P.O. Box 646340, Pullman, WA 99164-6340, USA*
[b] *School of Chemical Engineering and Bioengineering, Washington State University, P.O. Box 642710, Pullman, WA 99164-2710, USA*

Received 24 January 2007; received in revised form 16 April 2007
Available online 11 June 2007

This article is dedicated to the memory of Reinhart Heinrich, one of the founding fathers of metabolic control theory and a pioneer of systems biology.

Abstract

To support their sessile and autotrophic lifestyle higher plants have evolved elaborate networks of metabolic pathways. Dynamic changes in these metabolic networks are among the developmental forces underlying the functional differentiation of organs, tissues and specialized cell types. They are also important in the various interactions of a plant with its environment. Further complexity is added by the extensive compartmentation of the various interconnected metabolic pathways in plants. Thus, although being used widely for assessing the control of metabolic flux in microbes, mathematical modeling approaches that require steady-state approximations are of limited utility for understanding complex plant metabolic networks. However, considerable progress has been made when manageable metabolic subsystems were studied. In this article, we will explain in general terms and using simple examples the concepts underlying stoichiometric modeling (metabolic flux analysis and metabolic pathway analysis) and kinetic approaches to modeling (including metabolic control analysis as a special case). Selected studies demonstrating the prospects of these approaches, or combinations of them, for understanding the control of flux through particular plant pathways are discussed. We argue that iterative cycles of (dry) mathematical modeling and (wet) laboratory testing will become increasingly important for simulating the distribution of flux in plant metabolic networks and deriving rational experimental designs for metabolic engineering efforts.

Keywords: BioPathAt; Bondomer; Cumomer; Elementary modes; Flux; Isotopomer; Metabolic control analysis

Contents

* Corresponding author. Tel.: +1 509 335 3794; fax: +1 509 335 7643.
E-mail address: lange-m@wsu.edu (B.M. Lange).
URL: http://www.wsu.edu/~lange-m/ (B.M. Lange).

0031-9422/$ - see front matter © 2007 Elsevier Ltd. All rights reserved.
doi:10.1016/j.phytochem.2007.04.021

1. Introduction

Metabolic engineering aims to purposefully alter (using genetic engineering techniques) an organism's metabolic pathways in order to better understand how these pathways work or to redesign them for the production of particular target metabolites. In 2002, the entire January issue of the journal *Metabolic Engineering* (Metabolic Engineering, Volume 4, Issue 1, Pages 1–106, January 2002) was devoted to highlighting the progress, problems and prospects of plant metabolic engineering. Undoubtedly, the plant metabolic engineering community has made considerable progress, which is attested by highly publicized success stories such as the development of provitamin A-producing grains of 'golden rice' (Ye et al., 2000) or the production of thermoplastic polyhydroxyalkanoate polymers in transgenic oilseed rape (Slater et al., 1999). However, further success of plant metabolic engineering at a commercial scale, besides suffering from lack of public acceptance in some parts of the world, has been hampered by an insufficient understanding of the mechanisms controlling flux through plant metabolic pathways, and the outcome of metabolic engineering attempts cannot yet be predicted with satisfactory accuracy (DellaPenna, 2001). With the advent of 'omics' technologies (in particular transcriptomics, proteomics, and metabolomics), which allow the global profiling of the abundance of constituents involved in metabolic pathways, our ability to document changes brought about by metabolic engineering is greatly enhanced. However, it has been argued that these approaches have to be augmented by quantitative mathematical modeling, combined in an iterative cycle with experimental testing of model predictions, to enable a rational design of metabolic engineering strategies (Sweetlove and Fernie, 2005; Fernie et al., 2005; Lange, 2006; Ratcliffe and Shachar-Hill, 2006). Pathway modeling has been an area of strength for chemical and biochemical engineers but most plant biologists are not familiar with the underlying mathematical framework. In this article, we are discussing some the most widely used methods for modeling metabolic networks and illustrate their utility in simplified case studies. We are attempting to provide sufficient information for phytochemists, biochemists, biophysicists and geneticists to understand the basic concepts of mathematical modeling and to allow them to evaluate the available literature. It is our hope that this article will serve as a primer for readers to think about how mathematical modeling can be utilized in providing quantitative descriptions of metabolic network behavior. Of course, we cannot cover the issue in-depth and the reader is referred to the primary literature and several excellent books for further perusal (Heinrich and Schuster, 1996; Fell, 1997; Stephanopoulos et al., 1998).

Various bioinformatic tools are available to compute the topology of genome-scale metabolic networks from experimental data (reviewed in Xia et al., 2004). However, the mathematical modeling methods used today for estimating flux through metabolic pathways (or networks of pathways) require an in-depth knowledge of one or more of the following input data: the (assumed) stoichiometry of all biochemical reactions, reversibility of enzymatic steps, branching patterns of (sub)pathways, uptake rates of a metabolic substrate and conversion rate into end products, subcellular compartmentation, the kinetic constants of the enzymes involved, and possibly profiles of transcript, protein and/or metabolite abundance. Thus, although genome-scale reconstructions have been attempted for microbes (reviewed in Price et al., 2004), the majority of flux modeling efforts in plants has been restricted to one pathway or a small set of pathways. Mathematical modeling approaches for flux determination can be categorized based on the algorithms, constraints and data types that are utilized, and their selection for a particular project will

Table 1
Overview of freely available software packages and online tools for mathematical modeling of plant metabolism

Modeling method	Software tool	References
Isotope labeling-based metabolic flux	13C-Flux	Wiechert et al. (2001)
	FiatFlux	Zamboni et al. (2005)
	Mathematica-based program (no name given)	Selivanov et al. (2006)
	NMR2Flux	Sriram et al. (2004)
Elementary modes analysis	FluxAnalyzer	Klamt et al. (2003)
	SNA	Urbanczik (2006)
	YANA	Schwarz et al. (2005)
Extreme pathway analysis	FluxAnalyzer	Klamt et al. (2003)
	Expa	Bell and Palsson (2005)
Kinetic modeling	CellDesigner (latest version is 3.5.1)	Funahashi et al. (2003)
	Cellware (latest version is 3.0.2)	Dhar et al. (2004)
	COPASI (latest version is 4.0)	Hoops et al. (2006)
	Dizzy (latest version is 1.11.4)	Ramsey et al. (2005)
	Dynetica (latest version is 2.0beta)	You et al. (2003)
	E-CELL 2	Takahashi et al. (2003)
	GEPASI (latest version 3.30)	Mendes (1993)
	JDesigner/Jarnac (latest version is 2.0.35)	http://sbw.kgi.edu/
	JSim	http://nsr.bioeng.washington.edu/PLN/Software
	JWS Online	Olivier and Snoep (2004)
	METATOOL 5.0	von Kamp and Schuster (2006)
	PLAS (Power Law Analysis and Simulation)	http://www.dqb.fc.ul.pt/docentes/aferreira/plas.html
	PySCeS	Olivier and Snoep (2004)
	Systems Biology Toolbox for MATLAB	Schmidt and Jirstrand (2006)
	Vcell (latest version is 4.2)	http://www.nrcam.uchc.edu/
	WebCell (latest version is 3.0)	Lee et al. (2006)
Reporting standards and repositories	BioModels	Le Novere et al. (2006)
	MFAML	Yun et al. (2005)
	MIRIAM	Le Novere et al. (2005)
	JWS Online	Olivier and Snoep (2004)
	SBML	SBML Forum (2003)
	WebCell (latest version is 3.0)	Lee et al. (2006)

depend on which prior experimental information is available.

The conceptually simplest method of metabolic flux analysis is the stoichiometric approach, which requires only very limited experimental data; essentially, only the topology of the network, the rate of uptake of a substrate, its conversion rate into products, and the production of biomass are considered. Further developments of this concept, which are based on the use of different algorithms and constraints, are flux balance analysis (FBA), extreme pathway analysis (EPA) and elementary modes analysis (EMA). Because of the limitations of stoichiometric modeling, an experimental approach was developed that is based on labeling experiments with stable isotopes (primarily ^{13}C) and subsequent analysis of the distribution of label in different carbon atoms of the target metabolites. Mechanistic (kinetic) models incorporate knowledge regarding the kinetic properties of enzymes involved in a metabolic network and can be used to simulate how intracellular fluxes will change when the experimental system is perturbed. Metabolic control analysis (MCA) has become the most widely used kinetics-based tool to gain a quantitative understanding of metabolic networks. In the following paragraphs we will discuss the different mathematical modeling approaches and will highlight progress made in applying these different approaches to understanding the control of plant metabolism. In Table 1 an overview of freely available software packages and online tools relevant to the mathematical modeling of plant pathways is presented. A critical assessment of these tools is beyond the scope of this article; for an excellent article evaluating tools for kinetic modeling the reader is referred to Alves et al. (2006). Since we will not be able to discuss every paper that has appeared in the field of mathematical modeling of plant pathways in this review article, we are providing a comprehensive listing (sorted by modeling approach and scientific area) in Table 2 and focus on the discussion of selected articles in the text.

2. Metabolic flux analysis

In metabolic flux analysis (MFA) intracellular fluxes are calculated by using a stoichiometric model for the major intracellular reactions and applying mass balances around intracellular metabolites. This concept is based upon the fundamental law of mass conservation (all mass inputs into a metabolic network must be recovered, transformed or remain unchanged; Heinrich and Schuster, 1996). We distinguish between purely stoichiometric approaches (only a limited number of metabolite measurements are made; discussed in Sections 2.1 and 2.2) from those that utilize isotope labeling experiments (discussed in Section 2.3).

Ordinarily, the number of reactions (fluxes) is greater than the number of intracellular metabolites and the solution of metabolite balancing equations (a system of ordinary differential equations (ODEs) used as a mathematical framework to determine flux) will allow an infinite number of possible solutions (combination of fluxes). This is referred to as an under-determined system. Additional experimental measurements and derived constraints can be used to reduce the number of unknown fluxes. As a final step it is possible to introduce optimization criteria (e.g.,

Table 2
Overview of mathematical modeling papers focusing on plant metabolism

Modeling method	Pathway	Comment	References
Isotope labeling-based metabolic flux analysis	Central carbon metabolism	Quantification of compartmented metabolic fluxes in maize root tips	Dieuaide-Noubhani et al. (1995)
		In vivo pyruvate synthesis in maize roots was evaluated using a precursor-product	Edwards et al. (1998)
		Heterotrophic tobacco callus lines expressing a rat liver 6-phosphofructo-2-kinase/fructose-2,6-bisphosphatase were used to calculate rates of glucose metabolism	Fernie et al. (2001)
		Calculation of 18 fluxes of central metabolism based on (13)C enrichments in tomato suspension cultures	Rontein et al. (2002)
		Analysis of central metabolism in *Brassica napus* embryos based on (13)C enrichments in storage lipids and proteins	Schwender and Ohlrogge (2002)
		Quantitative metabolic flux model for the reaction network of glycolysis and the oxidative pentose phosphate pathway in *Brassica napus* embryos	Schwender et al. (2003)
		Based on isotopomer abundances in soybean seed storage protein and starch hydrolysates, fluxes through pathways of central carbon metabolism were calculated	Sriram et al. (2004)
		Flux contributions via several pathways of central carbon metabolism were estimated based on feeding labeled glucose to tobacco	Ettenhuber et al. (2005a)
		Relative flux contributions by different pathways of primary metabolism in maize kernels were determined by simulation of the isotopolog space of glucose	Ettenhuber et al. (2005b)
		A new futile cycle (glucose phosphate to glucose) was discovered that consumes about 40 % of all ATP generated in maize root tips	Alonso et al. (2006)
		Metabolism in tuber discs (response to low temperature) was monitored by determining the redistribution of radiolabel following incubation in [U-(14)C]glucose	Malone et al. (2006)
		(13)C-labeling experiments using glucose were carried out with kernels of maize inbred lines, heterotic hybrids, and starch-deficient mutants	Spielbauer et al. (2006)
	Choline metabolism	Conversion of [(33)P]phospho-ethanolamine, [(33)P]phosphomonomethylethanolamine, or [(14)C]formate into choline in tobacco leaf disks	McNeil et al. (2000a)
		Definition of constraints on glycine betaine synthesis based on [(14)C]choline labeling experiments and in vivo (31)P NMR analyses of tobacco leaf disks	McNeil et al. (2000b)
	Mitochondrial metabolism	Mitochondrial fluxes were determined after labeling Brassica napus embryos with (13)Cglucoses, (13)Calanine, (13)Cglutamine,	Schwender et al. (2006)
	Phenylpropanoid metabolism	Modulation of phenylpropanoid metabolism in wound-healing potato tuber tissue	Matsuda et al. (2003)
		Investigation of the metabolic pathways in *Petunia hybrida* petals leading from phenylalanine to benzenoid compounds	Boatright et al. (2004)
		Analysis of the effects of beta-1,3-oligosaccharide elicitor on the metabolism of phenylpropanoids in potato tuber	Matsuda et al. (2005)

(*continued on next page*)

Table 2 (*continued*)

Elementary modes analysis	C3 photosynthesis	Analysis of photosynthate metabolism in the chloroplast	Poolman et al. (2003)
	Central carbon metabolism	All possible routes of futile cycling of sucrose in sugar cane culm were enumerated; the available kinetic data for the pathway enzymes were then used a kinetic model	Rohwer and Botha (2001)
		Measurements of mass balance, Rubisco enzyme activity, stable isotope labelling and analysis of elementary flux modes (*Brassica napus* embryos)	Schwender et al. (2004b)
Kinetic modeling	C3 photosynthesis	Biochemical model of photosynthetic CO_2 assimilation in leaves of C3 species	Farquhar et al. (1980)
		Dynamic model of photosynthesis	Gross et al. (1991)
		Sensitivity of C3 photosynthesis to increasing CO_2 concentration	Kirschbaum (1994)
		Modeling of photosynthesis in fluctuating light (incl. stomatal conductance, biochemical activation and pools of key photosynthetic intermediates)	Kirschbaum et al. (1997)
		Estimation of carbon gain in sunfleck light regimes	Pearcy et al. (1997)
		Improvement of a previous kinetic model for the Calvin cycle and starch production	Pettersson (1997)
		Photosynthetic carbohydrate formation in C3 plants under conditions of light and carbon dioxide saturation	Pettersson and Ryde-Pettersson (1988)
		Flux control of the malate valve in leaf cells	Fridlyand et al. (1998)
		Oscillations in photosynthesis caused by changes in the ATP/ADP ratio or modulation of the pH gradient across the plastidial envelope membrane	Fridlyand (1998)
		Regulation of the Calvin cycle	Fridlyand and Scheibe (1999)
	C4 photosynthesis	Prediction of net photosynthesis and stomatal conductance from leaves of C4 plants	Collatz et al. (1992)
		Mechanistic leaf photosynthesis model for C4 grasses	Chen et al. (1994)
		Experimental data using *Zea mays* at different stages of development were analyzed using mathematical models of C4 photosynthesis	He and Edwards (1996)
		Computer model comprising light reactions in PS II and PS I, electron-proton transport reactions in mesophyll and bundle sheath chloroplasts	Laisk and Edwards (2000)
	CAM photosynthesis	Simulation of crassulacean acid metabolism	Nungesser et al. (1984)
		Model of crassulacean acid metabolism describing the varying concentrations of pools of major metabolites by a system of coupled nonlinear differential equations is proposed	Blasius et al. (1997)
		Hysteresis switch in an oscillatory model of crassulacean acid metabolism	Neff et al. (1998)
		Oscillatory model of crassulacean acid metabolism describing the CO_2 uptake and nocturnal acidification	Blasius et al. (1998)
		Non-linear theoretical model of mechanism of endogenous circadian photosynthesis oscillations of plants performing crassulacean acid metabolism	Blasius et al. (1999)
	Central carbon metabolism	Regulation of several enzymes in central carbon metabolism as a response to hypoxia in maize root tips	Roscher et al. (1998)
		Kinetic model of the branchpoint between methionine and threonine biosynthesis	Curien et al. (2003)
		Analysis of central carbon metabolism in *Catharanthus roseus* hairy root cultures	Leduc et al. (2006)
	Carotenoid metabolism	Kinetic model of the xanthophyll cycle	Sielewiesiuk and Gruszecki (1991)
		Kinetics of the two de-epoxidation steps occurring in the xanthophyll cycle	Latowski et al. (2000)

(*continued on next page*)

Table 2 (*continued*)

Modeling method	Pathway	Comment	References
Kinetic modeling	Choline metabolism	Modeling of choline metabolism in transgenic plants	McNeil et al. (2000b)
		Modeling of choline metabolism in transgenic plants	Nuccio et al. (2000)
	Isoprene emission	Model describing the formation of isoprene in oak under varying environmental conditions	Zimmer et al. (2000)
	Mitochondrial respiration	Modeling of the respiratory network in plant mitochondria	Krab (1995)
	Redox regulation	Dissection of the superoxide dismutase-ascorbate-glutathione pathway in chloroplasts	Polle (2001)
Metabolic control analysis	C3 photosynthesis	Simulation of dynamic and steady-state behavior of the Calvin cycle reactions of the chloroplast, including starch synthesis and degradation, and triose phosphate export	Poolman et al. (2000)
		Regulation of fluxes in transgenic plants with reduced activities of Calvin-cycle enzymes	Fridlyand and Scheibe (2000)
		Analysis of mutants of phosphoglucose isomerase in the cytosol and chloroplast of *Clarkia xantiana*	Kruckeberg et al. (1989)
		Analysis of glycolysis in aged disks of tuber tissue from transgenic potatoes expressing different amounts of phosphofructokinase	Thomas et al. (1997a)
		Distribution of glycolytic flux control between the steps of glycolysis in aged disks of potato tuber under aerobic conditions	Thomas et al. (1997b)
		Control of gluconeogenesis in endosperm from 4-day-old castor bean seedlings	Runquist and Kruger (1999)
		Kinetic model of the branchpoint between methionine and threonine biosynthesis	Curien et al. (2003)
	Biopolymer production	Prospects of producing the copolymer poly-(3-hydroxybutyrate-co-3-hydroxyvalerate) in plant plastids	Daae et al. (1999)
	Carotenoid metabolism	Evaluation of transgenic tomato plants expressing an additional phytoene synthase in a fruit-specific manner	Fraser et al. (2002)
	Glutamine synthetase/ glutamate synthase cycle	Metabolic control analysis of the glutamine synthetase/glutamate synthase cycle of barley chloroplasts	Baron et al. (1994)
	Lipid metabolism	The importance of acetyl-CoA carboxylase in regulation of lipid synthesis for barley and maize leaves was quantitatively assessed using inhibitor titration studies	Page et al. (1994)
		Analysis of de novo fatty acid biosynthesis in developing sunflower seeds	Martinez-Force and Garces (2000)
		Study of consequences of omega -6-oleate desaturase deficiency on mitochondrial membrane function in *Arabidopsis thaliana*	Caiveau et al. (2001)
		Analysis of lipid biosynthesis in tissue cultures from oil cropsa (olive, oil palm)	Ramli et al. (2002)
		Analysis of lipid biosynthesis in tissue cultures from oil cropsa (olive, oil palm)	Ramli et al. (2005)
	Redox regulation	Analysis of glutathione (GSH) and phytochelatin synthesis	Mendoza-Cózatl and Moreno-Sánchez (2006)
	Mitochondrial respiration	Analysis of the control of phosphorylation-coupled respiration in isolated plant mitochondria	Padovan et al. (1989)

the network strives to produce a certain essential metabolite at highest possible concentrations), which allows linear programming (a well-developed mathematical approach for solving diverse optimization problems) to be applied for solving the system of ODEs.

2.1. Case study of flux balance analysis

Stoichiometric analyses require knowledge about the (assumed) topological structure of the metabolic network under consideration and assume that the network operates

at a pseudo-steady state (the macroscopic variables – flux and metabolite concentrations – change only to a tolerable extent over a specific time span) (Heinrich and Schuster, 1996; Schilling et al., 1999; Klamt and Stelling, 2003). For the simultaneous solution of mass balance equations, a homogeneous system of linear algebraic equations is set up to define a vector of metabolite concentrations $\boldsymbol{M}$, a stoichiometric matrix $\boldsymbol{S}$, of order $\boldsymbol{m} \cdot \boldsymbol{n}$ ($\boldsymbol{m}$, number of pathway metabolites; $\boldsymbol{n}$, number of metabolic fluxes), and a vector $\boldsymbol{v}$ of net reaction rates. The variation of a metabolite concentration over time ($\mathrm{d}\boldsymbol{M}/\mathrm{d}t$) is proportional to the rate of reaction at which it is synthesized minus the rate of reaction at which it is consumed. At steady state conditions the following expression is obtained:

$$\frac{\mathrm{d}\boldsymbol{M}}{\mathrm{d}t} = S \cdot v = 0.$$

We will now use a simple example to illustrate the use of flux balance analysis (FBA). Let us consider the metabolic network defined in Scheme 1.

A plant cell imports the metabolite $\boldsymbol{A}_{\mathrm{ext}}$ from the apoplastic space (the internal metabolite is referred to as $\boldsymbol{A}$). The metabolic network consists of two reactions that result in the formation of metabolites $\boldsymbol{B}$ and $\boldsymbol{C}$. These cytosolically synthesized metabolites are then transported to plastids (they are now referred to as $\boldsymbol{B}_{\mathrm{plast}}$ and $\boldsymbol{C}_{\mathrm{plast}}$) and associate with thylakoids. Our purpose is to determine the internal flux distribution, using FBA, in the subnetwork circumscribed by the blue oval of Scheme 1.

The metabolic reactions and transport processes can be summarized as follows ($\boldsymbol{v}_i$ are reaction rates, $\boldsymbol{b}_i$ are transport rates):

$$\boldsymbol{A} \xrightarrow{\boldsymbol{v}_1} \boldsymbol{B}, \tag{1}$$

$$\boldsymbol{A} \xrightarrow{\boldsymbol{v}_2} \boldsymbol{C}, \tag{2}$$

$$\boldsymbol{B} \xrightarrow{\boldsymbol{v}_3} \boldsymbol{C}, \tag{3}$$

$$\boldsymbol{A}_{\mathrm{ext}} \xrightarrow{\boldsymbol{b}_1} \boldsymbol{A}, \tag{4}$$

$$\boldsymbol{B} \xrightarrow{\boldsymbol{b}_3} \boldsymbol{B}_{\mathrm{plast}}, \tag{5}$$

$$\boldsymbol{C} \xrightarrow{\boldsymbol{b}_2} \boldsymbol{C}_{\mathrm{plast}}. \tag{6}$$

The mass balance of a metabolite (variation over time $\mathrm{d}\boldsymbol{M}/\mathrm{d}t$) is defined as the difference between the rate(s) of production and the rate(s) of consumption. Applied to all metabolites in our network, the following set of coupled ODEs can be formulated (Scheme 2). We have now defined the metabolic network and have derived the corresponding dynamic mass balance equations, which can also be rewritten in matrix notation (Scheme 3). To calculate the flux distribution in the network under consideration, we need to identify imposed restrictions (constraints) to the system. If we consider that the macroscopic variables (metabolite concentrations and fluxes) do not change considerably over a certain time span (steady-state assumption), the dynamic mass balance equations can be represented as $\boldsymbol{S} \cdot \boldsymbol{v} = 0$, where $\boldsymbol{S}$ is the stoichiometric matrix and $\boldsymbol{v}$ the flux vector.

The arrows in Scheme 3 indicate which flux in the flux vector corresponds to which stoichiometric coefficient in the first line of the stoichiometric matrix based on the first equation (specifying $\mathrm{d}A/\mathrm{d}t$) in Scheme 2. Lines 2 and 3 of the stoichiometric matrix are obtained in the same way for $\mathrm{d}B/\mathrm{d}t$ and $\mathrm{d}C/\mathrm{d}t$, respectively. For our example the number of unknown fluxes ($\boldsymbol{v}_1, \boldsymbol{v}_2, \boldsymbol{v}_3, \boldsymbol{b}_1, \boldsymbol{b}_2$, and $\boldsymbol{b}_3$) is greater than the number of metabolites ($\boldsymbol{A}$, $\boldsymbol{B}$, and $\boldsymbol{C}$), which means that the steady-state solution of fluxes is under-determined. Thus, additional constraints such as measurable metabolite concentrations and measurable fluxes can be used to uniquely determine the flux distribution. Let us assume that we have measured the concentrations of metabolites $\boldsymbol{A}_{\mathrm{ext}}$ and $\boldsymbol{A}$ over a certain period of time; we then calculate the uptake rate $\boldsymbol{b}_1$ (for this example we assume this rate is in the range of up to 10 pmol (g fresh weight s)$^{-1}$). Let us also assume that we have measured the concentrations of metabolites $\boldsymbol{B}_{\mathrm{plast}}$ and $\boldsymbol{C}_{\mathrm{plast}}$ and we observed that their ratio under various conditions is always greater than or equal to 3:1. Further assumptions are that the cell under consideration is experiencing high light exposure and that compound $\boldsymbol{B}_{\mathrm{plast}}$ is an essential component of the high light response of plants, which should be synthesized at high levels under these conditions. In order to determine the internal flux distribution, we can thus formulate an objective function $\boldsymbol{Z}$ (the cell maximizes the produc-

$$\frac{dA}{dt} = b_1 - v_1 - v_2$$

$$\frac{dB}{dt} = v_1 - b_3 - v_3$$

$$\frac{dC}{dt} = v_2 + v_3 - b_2$$

Scheme 2. Dynamic mass balance equations.

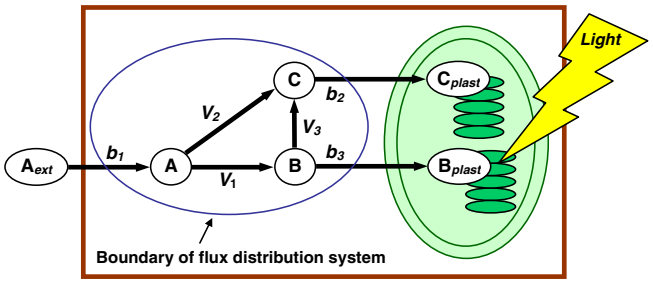

Scheme 1. Example network to illustrate flux balance analysis.

$$\frac{d}{dt}\begin{bmatrix} A \\ B \\ C \end{bmatrix} = \begin{bmatrix} -1 & -1 & 0 & 1 & 0 & 0 \\ 1 & 0 & -1 & 0 & 0 & -1 \\ 0 & 1 & 1 & 0 & -1 & 0 \end{bmatrix} \begin{bmatrix} v_1 \\ v_2 \\ v_3 \\ b_1 \\ b_2 \\ b_3 \end{bmatrix} = \begin{bmatrix} 0 \\ 0 \\ 0 \end{bmatrix}$$

Scheme 3. Mass balance equations in matrix form.

tion of $\boldsymbol{B}_{\text{plast}}$, and because $\boldsymbol{B}_{\text{plast}}$ and $\boldsymbol{C}_{\text{plast}}$ are linked as defined above, also $\boldsymbol{C}_{\text{plast}}$), which can be treated as a linear optimization problem:

$$\text{Maximize} \quad \boldsymbol{Z} = \boldsymbol{B}_{\text{plast}} + \boldsymbol{C}_{\text{plast}} = \boldsymbol{b}_2 + \boldsymbol{b}_3 \quad \text{Objective function.}$$

Summary of constraints:

(1) $\boldsymbol{S} \cdot \boldsymbol{v} = 0$ – Mass balance constraint assuming steady-state
(2) $b_1 \leqslant 10$ – Inferred by measurement of concentrations of $\boldsymbol{A}_{\text{ext}}$ and $\boldsymbol{A}$
(3) $\boldsymbol{b}_3 \geqslant 3 \cdot \boldsymbol{b}_2$ – Inferred by measurement of concentrations of $\boldsymbol{B}_{\text{plast}}$ and $\boldsymbol{C}_{\text{plast}}$
(4) $\boldsymbol{v}_1, \boldsymbol{v}_2, \boldsymbol{v}_3, \boldsymbol{b}_1, \boldsymbol{b}_2, \boldsymbol{b}_3 \geqslant 0$ – Assumption that all reactions and the direction of transport are not reversible

Optimization problems with an objective function are often times solved using an approach called linear programming. This method identifies one solution (in this case a maximum) that satisfies all constraints. One popular technique for the numerical solution of a linear programming problem is the simplex algorithm. Because of space limitations we cannot discuss all iterations of this process in this review article, but for those interested, the entire solution for our example is shown in Supplementary Material 1. The following optimal solution for the problem under consideration (fluxes are expressed in pmol (g fresh weight s)$^{-1}$) was obtained:

$$\boldsymbol{b}_1 = 10, \quad \boldsymbol{b}_2 = 2.5, \quad \boldsymbol{b}_3 = 7.5, \quad \boldsymbol{v}_1 = 7.5, \quad \boldsymbol{v}_2 = 2.5, \quad \boldsymbol{v}_3 = 0.$$

Optimizations for determining fluxes through metabolic pathways even of limited complexity (as in our example) are quite tedious. If a larger number of reactions is considered (or a network of pathways), then the solution has to be determined computationally.

2.1.1. Limitations of stoichiometric analyses

The key to a successful stoichiometric analysis is the judicious selection of constraints but its solution demands the experimental determination of unknown intracellular fluxes which might be difficult to quantify without further simplifications, restricting the reliability of the obtained fluxes. However, even if for a particular metabolic pathway the influx of a substrate and the efflux of an end product are known, there are several cases when stoichiometric MFA cannot predict flux distribution accurately: if (1) reversible reactions have to be considered, (2) parallel pathways exist or pathways occur in more than one compartment, (3) metabolic cycles are part of the metabolic network, (4) enzyme cofactors are not balanced, (5) pathways are compartmentalized, and/or (6) the steady-state assumption does not hold because of diurnal, seasonal or environmental fluctuations (Stephanopoulos et al., 1998; Varner and Ramkrishna, 1999; Wiechert, 2001). It is not unusual that one or more of these conditions apply in plants and that results with stoichiometric analyses are at best ambiguous (Roscher et al., 2000; Morgan and Rhodes, 2002). So why would we discuss FBA is such detail when its utility for modeling plant pathways (and networks of pathways) is very limited? In the upcoming paragraphs we will introduce other mathematical modeling approaches that use the same mathematical framework (constraint-based models using reaction stoichiometry) and in this article FBA serves as an introductory example of a balancing problem.

2.2. Metabolic pathway analysis

2.2.1. Elementary modes analysis

FBA assumes a certain topology for the metabolic network under consideration. In cases where numerous possibilities for flux distribution exist (e.g., branched pathways), FBA does not lead to unambiguous solutions. Several approaches for metabolic pathway analysis (MPA) have been developed that also build on constructing models based upon reaction stoichiometries but help to find unique solutions to determine flux distribution in metabolic networks. One of these methods is elementary modes analysis (EMA), in which elementary flux modes define the minimum set of reactions that can operate at steady-state under certain constraints and that cannot be further decomposed conceptually (Schuster and Hilgetag, 1994; Schuster et al., 1999; Stelling et al., 2002; Gagneur and Klamt, 2004). A complete and thus unique set of pathways, which represents all possible solutions that meet the constraints imposed on the metabolic network under consideration, is generated. The computational challenge that arises from such network decompositions is that, even for relatively simple pathways, thousands of elementary flux modes may have to be considered, particularly when nodes (metabolites) with high connectivities (involvement in numerous reactions) need to be considered. Stelling et al. (2002) introduced an approach to calculate 'control-effective fluxes', which assigns an 'efficiency' to each elementary mode to relate its output (enhanced growth, production of energy equivalents, increased photosynthetic rate) to the bioenergetic investment required (synthesis of enzymes). Then, the determined fluxes are weighted by each mode's efficiency, which leads to the generation of control-effective fluxes. Rohwer and Botha (2001) used EMA to outline viable pathways for the futile cycling of sucrose in sugar cane culm (Fig. 1). Earlier feeding experiments with labeled isotopes had shown that significant futile cycling occurred in sucrose-accumulating sugar cane, which was hypothesized to be a limiting factor in sucrose accumulation (Whittaker and Botha, 1997). Interestingly, EMA revealed that the first 5 of the 14 modes shown in Fig. 1 represented futile cycles, which do not result in the accumulation of an end product (Rohwer and Botha, 2001). Modes 6–8 exemplify the utilization of hexoses to provide precursors for glycolysis. Modes 9, 10, 12 and 13 lead to the accumulation of sucrose in vacuoles using fructose as a precursor, whereas

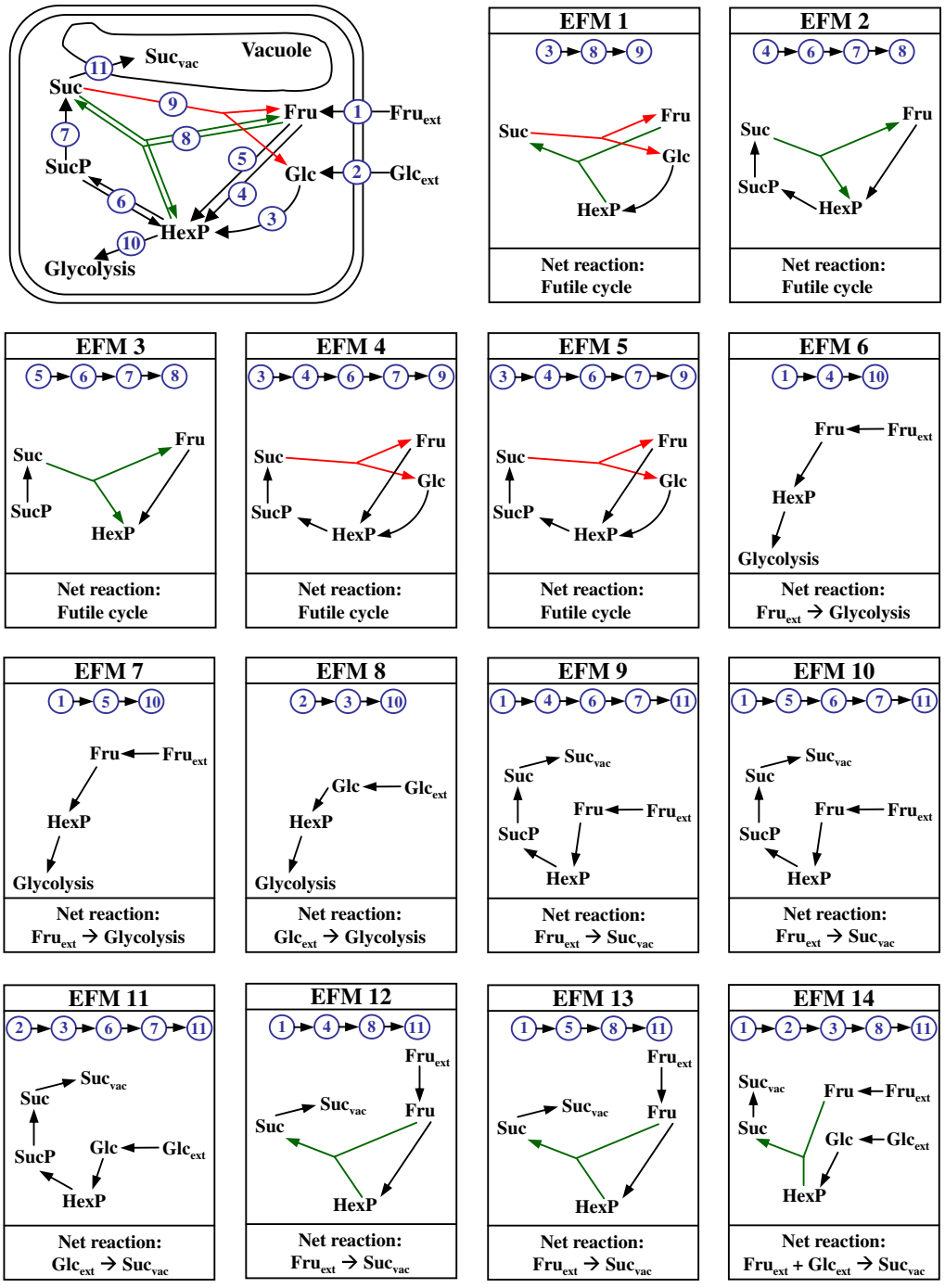

Fig. 1. Elementary modes analysis of sucrose metabolism in sugar cane culm (based upon data from Rohwer and Botha, 2001). *Abbreviations*: ext, external; Fru, fructose Glc, glucose; HexP, hexose phosphates; Suc, sucrose, SucP, sucrose phosphate; vac, vacuolar. For details see text.

mode 11 is based upon the metabolization of glucose. Mode 14 takes into account that both fructose and glucose can be used as precursors for sucrose biosynthesis. The information regarding possible pathways was then integrated with data obtained using a modeling approach that accounts for the kinetic and thermodynamic properties of the enzymes involved in the sucrose accumulation network (for details regarding kinetic modeling see Section 3 of this review). Based on this integrative analysis the authors suggested a metabolic engineering strategy for enhancing sucrose accumulation by overexpression of either (1) the fructose importer, (2) the glucose importer, or (3) the vacuolar sucrose importer (in Fig. 1, these correspond to enzymes 1, 2 and 11, respectively). In addition to modulating enzymes involved in transport, the kinetic modeling also suggested that a reduction in the activity of invertase (enzyme 9 in Fig. 1) should be a viable strategy for increasing sucrose levels (Rohwer and Botha, 2001). The combination of EMA and kinetic modeling has allowed the authors to formulate hypotheses that can now be tested experimen-

tally. Poolman et al. (2003) applied EMA to investigate feasible pathways of central carbon metabolism in the chloroplast stroma (in particular the Calvin cycle, the oxidative pentose phosphate pathway and triose phosphate transport) under different light conditions. Based upon these analyses, Calvin cycle reactions, the oxidative pentose phosphate pathway and the thioredoxin system are combined to break down transitory starch for the synthesis of triose phosphates. The authors also propose that in the dark the oxidative pentose phosphate pathway operates cyclically and leads to the formation of C3, C4 and C5 but, unexpectedly, not C6 sugar phosphates. Schwender et al. (2004b) performed an EMA analysis of oil biosynthesis (from glucose to fatty acids) in developing oilseed rape embryos to evaluate the contribution of various alternative pathways. In combination with isotope labeling experiments and enzyme activity measurements, these studies demonstrated that carbon fixation in these seeds operates in the absence of a Calvin cycle, which was shown to increase the carbon use efficiency by combining the activity of Rubisco with the non-oxidative reactions of the pentose phosphate pathway. Compared to a conversion of hexose phosphates through glycolysis this newly discovered route increases the acetyl-CoA production from hexose phosphates by 20% and reduces the loss of CO_2 (produced by pyruvate dehydrogenase) by 40%. This might explain why developing seeds of numerous plants have high Rubisco but negligible Calvin cycle activities.

2.2.2. Extreme pathway analysis

Another approach for MPA utilizes the concept of convex analysis, which identifies a unique set of 'extreme pathways' that define the topology of the metabolic network under consideration (Schilling et al., 2000, 2001; Papin et al., 2002; Price et al., 2003). Every steady-state flux can be expressed as a non-negative linear combination of these extreme pathways. A limitation of extreme pathway analysis (EPA) relates to the fact that the number of extreme pathways increases exponentially with the size of the network under consideration. Thus, this approach has been applied to networks of reduced size (division into subsystems) or complexity (focus on a particular process altered by an experimental treatment) (reviewed in Price et al., 2003). Network analyses to evaluate the topological properties of plant metabolic networks have been performed for metabolic pathways in plastids (Wang et al., 2006) and it is conceivable that EPA could be employed successfully for specific pathways (e.g., the Calvin cycle and its branchpoints leading into central carbon metabolism) within such a network. In fact it would be quite interesting to assess the outcome of such an analysis in light of the published studies using EMA.

2.3. Case study of isotope labeling-based metabolic flux analysis

Steady-state isotope labeling-based MFA has been employed successfully when reversible enzymatic steps, metabolic cycles and/or subcellular compartmentation have to be considered for a particular metabolic network of interest (for recent reviews see Roscher et al., 2000; Giersch, 2000; Wiechert, 2001; Morgan and Rhodes, 2002; Schwender et al., 2004a,b; Wiechert and Nöh, 2005; Ratcliffe and Shachar-Hill, 2006). The choice of the labeled precursor is of paramount importance as feeding with different isotopomers (metabolites containing an isotopic atom in different positions) may lead to differences in the labeling patterns of the constituents of a metabolic network. The isotopically labeled precursor is supplied continuously until the pool sizes and labeling patterns of all metabolites remain essentially constant (metabolic and isotopic steady-state). The proportion of isotope-labeled atoms in each metabolite (fractional enrichment) can then be quantified using radiotracer analysis (if radioisotopes are used), nuclear magnetic resonance (NMR; if isotopes such as ^{2}H, ^{13}C, ^{15}N or ^{31}P are used) or analytical techniques based on mass spectrometry (MS; applicable for all commonly used isotopes) (for reviews see Szyperski, 1998; Ratcliffe and Shachar-Hill, 2001). The advantages and disadvantages of using a particular technology for assessing fractional isotope enrichments are discussed in-depth in Szyperski (1998). Experimentally, fractional enrichments can be achieved using various different methods: (1) the substrate is isotope-labeled in one (or more) specific position(s) and the isotopic enrichment in cellular metabolite pools is monitored (positional labeling); (2) two different substrates, of which only one is isotope-labeled, are proffered and isotope enrichments are quantified (dilution of isotope enrichment); (3) a mixture of unlabeled and uniformly isotope-labeled substrate are supplied and the metabolic flux information is contained in the integrity of bonds formed (bond labeling); and (4) a combination of the above techniques (for more details see Roscher et al., 2000).

To illustrate the analysis of fractional enrichments and the estimation of metabolic fluxes, we will use a metabolic network very similar to that depicted in Scheme 1, with the difference that the reaction of $\boldsymbol{v}_2$ occurs in the opposite direction, thus resulting in a futile cycle with $\boldsymbol{v}_1$, $\boldsymbol{v}_2$ and $\boldsymbol{v}_3$ (Scheme 4). $\boldsymbol{A}_{ext}$ represents a six-carbon metabolite that is proffered as a mixture in unlabeled and U-^{13}C-labeled form. After uptake of $\boldsymbol{A}_{ext}$ into the cell, $\boldsymbol{A}$ is converted to the five-carbon metabolite $\boldsymbol{B}$ and the one-carbon metabolite $\boldsymbol{E}$. $\boldsymbol{B}$ is then cleaved to form the three-carbon metabolite $\boldsymbol{C}$ and the two-carbon metabolite $\boldsymbol{D}$. Both $\boldsymbol{B}$ and $\boldsymbol{C}$ can be transported to chloroplasts. Alternatively, the three-carbon metabolite $\boldsymbol{C}$ can react with $\boldsymbol{D}$ and $\boldsymbol{E}$ to complete a metabolic cycle and regenerate $\boldsymbol{A}$.

2.3.1. Atom mapping matrices

First, we are going to discuss the steps to derive the principal equations for modeling isotope distributions which can then be used to estimate metabolic fluxes. An important advance was the introduction of the concept of atom

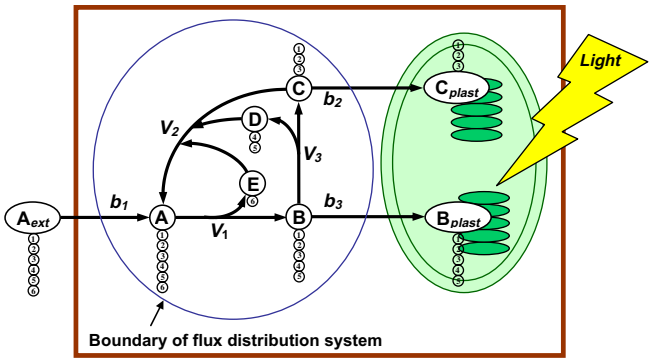

Scheme 4. Example network to illustrate the isotopomer and cumomer approaches to metabolic flux analysis.

mapping matrices (AMMs), which describe the transfer of atoms from reactants to products, thus resulting in a mapping matrix for each reactant–product pair (Zupke and Stephanopoulos, 1994). This method starts with representing the degree of isotope enrichment of each metabolite in vector form (label distribution vector) (note that in the literature the terms 'metabolite vector' and 'metabolite specific activity vector' are also used):

$$A = \begin{bmatrix} A(1) \\ A(2) \\ A(3) \\ A(4) \\ A(5) \\ A(6) \end{bmatrix}, \quad B = \begin{bmatrix} B(1) \\ B(2) \\ B(3) \\ B(4) \\ B(5) \end{bmatrix}, \quad C = \begin{bmatrix} C(1) \\ C(2) \\ C(3) \end{bmatrix}$$

Label distribution vector.

Because we are proposing the use of a mixture of unlabeled and ^{13}C-labeled substrate in our hypothetical experiment, the three-carbon metabolite ***C*** can have eight different isotope labeling states (2^n isotopomers, where n is the number of carbons in the metabolite) (see Scheme 5).

The second step is then to derive the AMMs. For the metabolic network shown in Scheme 4, the following processes are considered when constructing AMMs (Scheme 6).

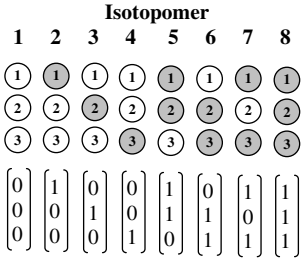

Scheme 5. Example showing all possible isotopomers of a three-carbon metabolite. Unlabeled atoms are depicted as hollow circles, whereas isotope-labeled atoms are shown as gray circles. The lower panel depicts labeling pattern formulated in vector notation.

We will now use reaction (6) from Scheme 6 as an example for constructing AMMs. In this notation $[C > A]_{Enz2}$ represents an atom mapping matrix that describes the transfer of carbon from metabolite ***C*** to metabolite ***A***, catalyzed by enzyme ***Enz2***; $[D > A]_{Enz2}$ describes the transfer of carbon from ***D*** to ***A***, also catalyzed by ***Enz2***; and $[E > A]_{E2}$ describes the transfer of carbon from ***E*** to ***A***, again catalyzed by ***Enz2***. The three carbon atoms of ***C*** will form the first three carbons of ***A*** (in matrix notation a "1" indicates that a particular carbon atom is transferred from a reactant to a product, whereas a "0" indicates that a specific carbon atom is derived from a different reactant). ***D*** will contribute carbons 4 and 5 to ***A***, and ***E*** will add the sixth carbon atom to the formation of ***A*** (Scheme 7). It is important to note that the AMMs do not contain information regarding the position of isotope label (which is specified by the label distribution vector); they just describe the transfer of carbon atoms from reactants to products.

As a third step, the metabolite labeling vector is multiplied by the appropriate AMM. By adding up the contributions of each reactant (product of AMM and the respective label distribution vector) modified by the corresponding reaction flux, we obtain the label distribution for the metabolic step specified in reaction (6) of Scheme 6:

$$A = [C > A]_{Enz2} C \cdot v_3 + [D > A]_{Enz2} D \cdot v_3 + [E > A]_{Enz2} E \cdot v_3.$$

If all reactions using ***A*** as a reactant and all reactions forming ***A*** as a product are combined (reactions (1), (2), and (6)

Reaction	Function / Notation
(1) $A_{ext} \rightarrow A$	*Transport*
(2) $A \xrightarrow{Enz1} B + E$	$[A > B]_{Enz1}$; $[A > E]_{Enz1}$
(3) $B \rightarrow B_{plast}$	*Transport*
(4) $B \xrightarrow{Enz3} C + D$	$[B > C]_{Enz3}$; $[B > D]_{Enz3}$
(5) $C \rightarrow C_{plast}$	*Transport*
(6) $C + D + E \xrightarrow{Enz2} A$	$[C > A]_{Enz2}$; $[D > A]_{Enz2}$; $[E > A]_{Enz2}$

Scheme 6. Construction of atom mapping matrices.

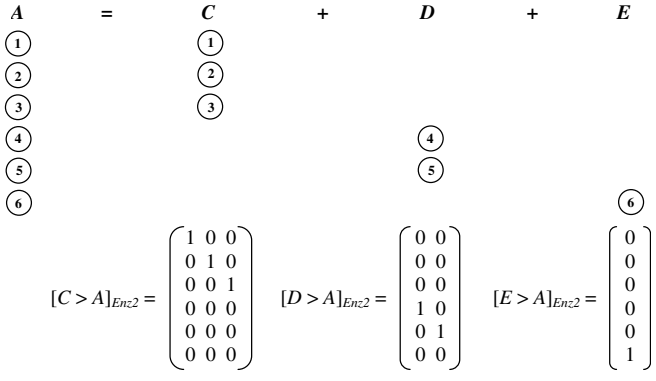

Scheme 7. Example of generating atom mapping matrices.

of Scheme 6), the following equation is obtained to describe label distribution:

$$b_1 + v_2\{[C > A]_{Enz2}C + [D > A]_{Enz2}D + [E > A]_{Enz2}E\} = v_1 \cdot A.$$

The steady-state isotope distribution for the entire metabolic network under consideration (Scheme 4) can be calculated from the simultaneous solution of the above equation and those specifying label distributions for ***B*** and ***C***. Using an iterative computational approach, unknown metabolic fluxes can be estimated and the equations describing isotope distributions solved. The calculated values are then compared with experimentally determined isotope enrichment data and the computational process is repeated until satisfactory convergence is reached, while still meeting all stoichiometric constraints (Zupke and Stephanopoulos, 1994; Stephanopoulos et al., 1998).

2.3.2. Isotopomer balancing

A further development of the AMM concept involves the use of isotopomer mapping matrices (IMMs) (Jeffrey et al., 1991; Schmidt et al., 1997), in which the expression of all isotopomer mass balances of a metabolite pool is achieved in a single matrix equation. In analogy to label distribution vectors of the AMM approach, IMMs use isotopomer distribution vectors (IDVs). Its notation is binary (hence the subscript 'bin') using a "0" for absence and a "1" for presence of isotope label. For metabolite ***A*** in the metabolic network depicted in Scheme 4 , the IDV $\boldsymbol{I_A}$ will contain $2^6 = 64$ elements (2^n isotopomers, where n is the number of carbons in the metabolite). The individual matrices shown in Scheme 7 are combined into one large matrix (Scheme 8).

The IDVs of product molecules are obtained by matrix multiplication of IMMs (which inform about the reaction mechanism) and IDVs of the reactants (Schmidt et al., 1997). IMMs contain all pairs of reactant isotopomers responsible for the synthesis of specific product isotopomers in all positions of the product IDV. Thus, IMMs can be used to identify the substrate isotopomer from which a specific product isotopomer was synthesized. There will be as many IMMs as the number of pairs of reactants and product molecules in a biochemical reaction (Schmidt et al., 1997). IMMs can be generated from AMMs in an iterative process, which we illustrate for reaction (6) of Scheme 6 in Supplementary Material 1. For a detailed explanation of the analytical solution and the interpretation of these results, see Schmidt et al. (1999).

$$I_A = \begin{bmatrix} I_A(1) \\ I_A(2) \\ I_A(3) \\ I_A(4) \\ \ldots\ldots \\ I_A(64) \end{bmatrix} = \begin{bmatrix} I_A(000000_{bin}) \\ I_A(000001_{bin}) \\ I_A(000010_{bin}) \\ I_A(000011_{bin}) \\ \ldots\ldots \\ I_A(111111_{bin}) \end{bmatrix}$$

Scheme 8. Example for generating isotopomer distribution vectors.

2.3.3. Cumomer balancing

Wiechert et al. (1999) developed an approach that simplifies the computational solution of balance equations where isotopomer variables are transformed into cumomer (*cum*ulated isotop*omer*) variables. Cumomers are "virtual molecules" defining a set of isotopomers. The notation used for cumomers uses a "1" for a labeled carbon atom and an "*X*" for an atom that is either labeled or unlabeled, which means that the binary notation of isotopomer balancing (e.g., C_{100bin}) becomes a positional notation (e.g., C_{1XX}). Cumomers can be combined into fractions (0-cumomer fraction for Cxxx; 1-cumomer fraction for C_{1XX}, C_{X1X}, C_{XX1}; 2-cumomer fraction for C_{11X}, C_{X11}, C_{1X1}; 3-cumomer fraction for C_{111}). In analogy to the example of the three-carbon metabolite isotopomers of Scheme 4, the cumomer fractions are depicted as follows (gray shading is used to indicate an isotope-labeled carbon, whereas gray and white stripes are used to indicate a carbon atom that is either isotope-labeled or not) (Scheme 9).

A novel framework for estimating flux distribution has been proposed (the elementary metabolite units (EMU) concept), which supposedly further simplifies the solution of isotopomer and cumomer equations; however, at the time of submission of this article only an abstract of the work was available online (Antoniewicz et al., 2007).

2.3.4. Bondomer balancing

The bondomer balancing concept includes, in addition to isotopomer distributions, information about carbon–carbon connectivity in metabolites. Bondomers of a metabolite differ in the number and positions of C–C bonds that remain intact after an isotope-labeled substrate enters a metabolic network (van Winden et al., 2002). An advantage of the bondomer balancing method over isotopomer balancing is that the number of required balance equations is lower, which makes bondomer balancing less computationally intense (van Winden et al., 2002). The bondomer balancing approach has been limited to experiments with [U-^{13}C]-labeled substrates (^{2}H or ^{15}N do not provide information about the integrity of C–C bonds). An expansion of this concept to include C–H or C–N bonds is conceivable but would require [U-^{13}C; U-^{2}H] or [U-^{13}C; U-^{15}N]-labeled

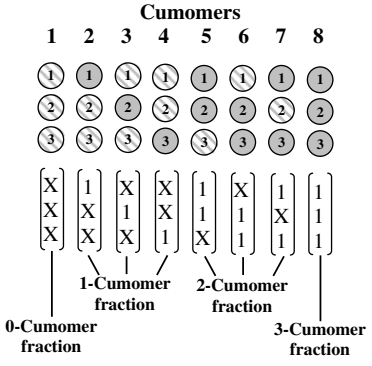

Scheme 9. Example showing all cumomers of a three-carbon metabolite.

substrates and would be computationally challenging. Bondomer distributions can be constructed in the same way as isotopomer distributions, except that the binary digits representing labeled or unlabeled states in isotopomer balancing represent the origin and integrity of C–C bonds in bondomer balancing. Scheme 10 illustrates the concept of evaluating bond integrity using the metabolic network example of Scheme 4.

In the reactions shown in Scheme 10 several bonds are broken and the atoms of the metabolites are regrouped in every cycle until the metabolic network reaches isotopic steady-state. Using two-dimensional ^{13}C NMR, the proportion of intact ^{13}C–^{13}C bonds in a particular metabolite can be determined. In analogy to isotopomer balancing, bondomer balancing uses the terms C–C bond mapping matrices (CCMMs), C–C bond vectors (CCVs), bondomer distribution vectors (BDVs) and bondomer mapping matrices (BMMs), which replace AMMs, label distribution vectors, IDVs and IMMs, respectively (van Winden et al., 2002). A new arithmetic approach for simulating bondomer distributions is based upon Boolean function mapping (Sriram and Shanks, 2004; Sriram et al., 2004). Using this method the topology of hypothetical pathways can be adjusted iteratively to match experimental isotopomer labeling results, thus allowing experimenters to test different pathway hypotheses.

2.4. Metabolic flux analysis for modeling of plant metabolic networks

Before attempting to conduct labeling experiments with subsequent mathematical modeling, it is important to understand to what extent the experimental design determines the possible outcomes. In principle, there are two types of isotope labeling approaches: whereas the transient approach requires sampling the time course as an isotopic label moves from an initial labeled substrate through the entire metabolic network, the steady-state approach is based upon a single measurement of labeled metabolic intermediates or end products at metabolic and isotopic steady-state. For metabolic networks that contain numerous reversible steps, futile cycles and/or enzymatic steps in different subcellular compartments (e.g., central carbon metabolism), the dynamic labeling approach is usually not well suited to investigate flux distributions and the steady-state approach should be employed. However, for networks of smaller size and reduced complexity the dynamic labeling approach can be very powerful (Matsuda et al., 2003; Boatright et al., 2004; Roessner-Tunali et al., 2004). It should be noted that the methods listed under Sections 2.3.1–2.3.4 apply only to steady-state modeling. For a more detailed discussion of the different isotope labeling approaches the reader is referred to an excellent recent review by Ratcliffe and Shachar-Hill (2006). In the upcoming paragraphs we are going to discuss examples from the literature to illustrate the complications when working with plant systems and highlight the success stories.

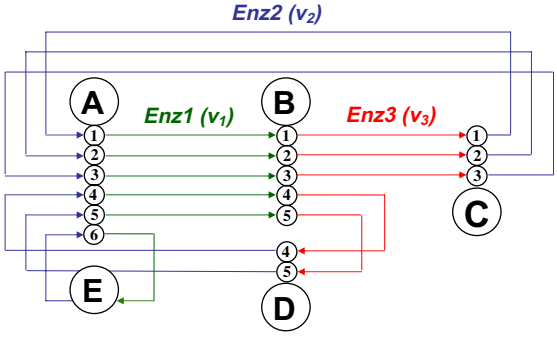

Scheme 10. Example of a bond-by-bond representation of the biochemical reaction network depicted in Scheme 4.

2.4.1. Steady-state labeling

Dieuaide-Noubhani et al. (1995) used [1-^{14}C]glucose as a substrate and the evolution of $^{14}CO_2$ (the production of CO_2 at steady-state is constant) as an end point measurement to determine when metabolic and isotopic steady-states were reached. Since under regular conditions CO_2 formation increased continuously, the authors "pre-starved" the root tips by incubating them in a medium that leads to a depletion of starch pools. Using this protocol a steady-state was reached after 10 h. Although this experimental trick rendered steady-state flux determinations feasible, it has to be questioned if such drastic treatments might displace the metabolic pathways studied by the authors from their usual steady-state. Thus, the fluxes determined by the authors might reflect metabolism under stress and could be quite different from those occurring in unstressed roots. Keeping this caveat in mind, the authors still provide valuable insights into the pathways utilized for the biosynthesis of particular cellular metabolite pools. Labeling with [1-^{14}C], [2-^{14}C] or [6-^{14}C]glucose revealed the importance of a plastid-localized pentose phosphate pathway for the formation of phospholipids and starch. Based on results obtained with feeding [1-^{13}C]glucose and analysis of ethanol extracts by ^{13}C NMR, it was concluded that cycling between hexose phosphates and triose phosphates occurred (resulting in randomization of label) and that a high turnover rate of sucrose (synthesis and degradation) in the cytosol was detectable. Further developments and expansions of this approach were later employed by the same group to investigate numerous central metabolic pathways during the growth cycle of tomato cell suspension cultures (Rontein et al., 2002). Roughly 30 fluxes were determined and allowed the authors to distinguish between pathways that appeared to be relatively resistant to changes in flux (e.g., glycolysis, pentose phosphate pathway, and the citric acid cycle) from those that reacted flexibly to flux alterations (e.g., various anabolic pathways). Edwards et al. (1998) extended these studies by measuring the ^{13}C fractional enrichment, using ^{13}C NMR and GC-MS, in glucose 6-phosphate, L-alanine, L-glutamate,

L-asparate and malate when [1-^{13}C]glucose was proffered to maize root tips grown. A simple precursor-product model allowed the authors to calculate the contributions of malic enzyme (EC 1.1.1.37), pyruvate kinase (EC 2.7.1.40) and phosphoenolpyruvate carboxylase (EC 4.1.1.31) to mitochondrial respiration. Fernie et al. (2001) studied heterotrophically grown tobacco callus cultures overexpressing a mammalian gene encoding 6-phosphofructo-2-kinase/fructose-2,6-bisphosphatase (EC 2.7.1.105/EC 3.1.3.46). This enzyme synthesizes fructose 2,6-bisphosphate, an allosteric regulator of the glycolytic enzyme fructose 1,6-bisphosphatase (EC 3.1.3.11) in photosynthetic tissues. Based on labeling experiments with [1-^{13}C]glucose and subsequent analysis of ethanol-soluble metabolite fractions by ^{1}H and ^{13}C NMR, increases in the rate of cycling of triose phosphates to hexose phosphates were observed in transgenic lines (correlating with fructose-2,6-bisphosphate levels), whereas the rate of sucrose cycling was not affected. Unexpectedly, metabolic conversions of [U-^{14}C]glucose or [U-^{14}C]glycerol into organic acids, amino acids and lipids in transgenic lines with increased fructose 2,6-bisphosphate levels, when compared to appropriate controls, were very similar (Fernie et al., 2001). Eisenreich and coworkers developed a ^{13}C NMR-based approach to evaluate labeling patterns following steady-state labeling with a combination of both isotope-labeled and unlabeled substrates; the results can be used to infer the biosynthetic origin of intermediates in central carbon metabolism (Glawischnig et al., 2001, 2002) and, thanks to the development of an improved computational analysis, has provided information about glucose recycling in tobacco plants (Ettenhuber et al., 2005a) and has provided evidence that, based on the analysis of kernels from genetically diverse maize lines, fluxes through central carbon metabolism are quite robust (Ettenhuber et al., 2005b; Spielbauer et al., 2006). Some of the most informative isotope labeling-based metabolic flux studies with plants were those aimed at elucidating the control of central carbon metabolism in embryos of oilseed rape (Schwender and Ohlrogge, 2002; Schwender et al., 2003, 2004a, 2006) which have been discussed in detail in a recent review (Ratcliffe and Shachar-Hill, 2006).

2.4.2. Dynamic labeling

The dynamic labeling approach was utilized to characterize changes in phenylpropanoid metabolism in potato tubers after wounding (Matsuda et al., 2003). The authors determined that the fluxes leading to *N*-*p*-coumaroyloctopamine (pCO) and chlorogenic acid (CGA), which are derived independently from a common precursor (*p*-coumaroyl-CoA), are not evenly distributed (4:1 flux ratio in favor of the pCO over the CGA branch). It was also shown that the breakdown rate of CGA was lower than that of pCO; because of its high turnover, pCO did not accumulate to high levels. The same approach was used in a follow-up paper studying the effect of oligosaccharide elicitor treatments on metabolic fluxes in potato tubers, which lead to a vastly increased flux into pCO (8.9-fold higher than in controls) and a decreased flux into CGA (2.7-fold lower than in controls) and metabolites derived from it (Matsuda et al., 2005). Despite the high pCO turnover rate, the elicitation resulted in a 25-fold transient increase in pCO levels. Boatright et al. (2004) studied a complex network of reactions metabolizing [$^{2}H_5$]phenylalanine to phenylpropanoids and benzenoids in excised petunia petals using the dynamic labeling approach. MFA revealed quantitative information about the branching of flux via CoA-dependent (β-oxidative) and CoA-independent (non-β-oxidative) pathways. A model prediction associated benzylbenzoate (BB), the role of which had not been previously defined, with the biosynthesis of benzoic acid and derived metabolites. The hypothesis that BB is a key intermediate in this pathway was substantiated by identifying and characterizing a petunia enzyme that catalyzes the formation of BB from benzoyl-CoA and benzyl alcohol. McNeil et al. (2000a) used mathematical modeling of [^{14}C] and [^{33}P] labeling data to determine the main route through the metabolic grid of choline (Cho) biosynthesis from ethanolamine in tobacco leaf disks. Follow-up work by the same group (McNeil et al., 2000b) assessed the role of compartmented fluxes (cytosolic, plastidial, vacuolar and apoplastic reaction were considered) in determining the fate of Cho with respect to its conversion into glycine betaine (in plastids). Based on computer simulations several constraints for glycine betaine accumulation were suggested: (1) small cytosolic Cho pool, (2) low capacity for phospho-Cho synthesis, (3) high Cho kinase activity and (4) low activity for Cho uptake into plastids. The first three constraints would limit precursor synthesis and all enzymes involved in this process had been characterized, whereas the fourth constraint indicated that an as yet unidentified transport activity might be important in the regulation of glycine betaine biosynthesis. This study provides an example of how experimentally testable hypotheses can be derived from predictions generated by mathematical modeling. The redistribution of radiolabel (from [U-^{14}C]glucose) and isotopic label (from [1-^{13}C]glucose) in potato tubers subjected to low temperatures was investigated by Malone et al. (2006). It was concluded that the increased sugar accumulation during cold storage, which renders tubers unsuitable for further processing, was not caused by the lability of certain enzymes as proposed in earlier works. Alonso et al. (2006) used pulse-labeling with [^{14}C]glucose to assess unidirectional rates of synthesis of major storage molecules (sucrose, starch and cell wall carbohydrates) and combined it with steady-state labeling using [1-^{13}C] and [U-^{13}C]glucose to quantify the extend of futile cycling in maize root tips. These studies identified a new glucose 6-phosphate to glucose cycle that is responsible for consuming a vast amount of ATP (roughly 40% of the total ATP). Enzyme assays confirmed the presence of substantial glucose 6-phosphate phosphatase activity in root tips.

2.4.3. Highlight: central carbon metabolism in soybean embryos

In the present review we are highlighting the development of an improved computational framework for the analysis of isotopomer abundances and its application to metabolic flux quantification in developing soybean embryos (Sriram et al., 2004). Labeling experiments of *in vitro* cultured, excised cotyledons were performed with a mixture of [U-^{13}C]glucose, glucose with natural ^{13}C abundance, and glutamine (Fig. 2). Storage protein and starch were extracted, hydrolyzed, and the resulting amino acids, sugars and derived hydrolyzates were subjected to analysis by two-dimensional [^{1}H, ^{13}C] NMR, primarily using the heteronuclear single quantum correlation (HSQC) pulse sequence. Assessment of cross peak intensities in NMR spectra and the evaluation of ^{13}C–^{13}C scalar coupling allowed isotopomeric abundances to be quantified for the aliphatic carbon atoms of 16 amino acids, the aromatic carbon atoms of phenylalanine, tyrosine and histidine, and for hexose sugars (which were detected as their hydrolysis products levulinic acid and hydroxyacetone) without prior purification of the analytes. Based on the available biochemical information in the literature, the authors reconstructed a model of the metabolic network involved in the synthesis of sink metabolites (amino acids that are integrated into storage proteins and sugar phosphates that are converted into transitory starch). If the pathway that is involved in converting a precursor into a sink end product was known, the NMR signal intensities measured for sink metabolites could be used to infer the expected isotopomeric composition of this precursor. By integrating the mathematical concepts of isotopomer balancing (described in Sections 2.3.2,2.3.3,2.3.4 of this review and references cited therein) with global optimization methods, Sriram et al. (2004) developed a computational tool, termed NMR2Flux, to convert isotopomer abundances into fluxes in an automated fashion. Fig. 2 summarizes these flux determinations for several steps of glycolysis (which is just an extract of the entire network considered by the authors). Forward and backward fluxes were calculated for steps depicted with gray reaction arrows in Fig. 2, although only the direction and values of total net fluxes are indicated. Sriram et al. (2004) were also able to distinguish between parallel fluxes in different compartments generated by isozyme activities (examples in Fig. 2 would be steps associated with the same EC num-

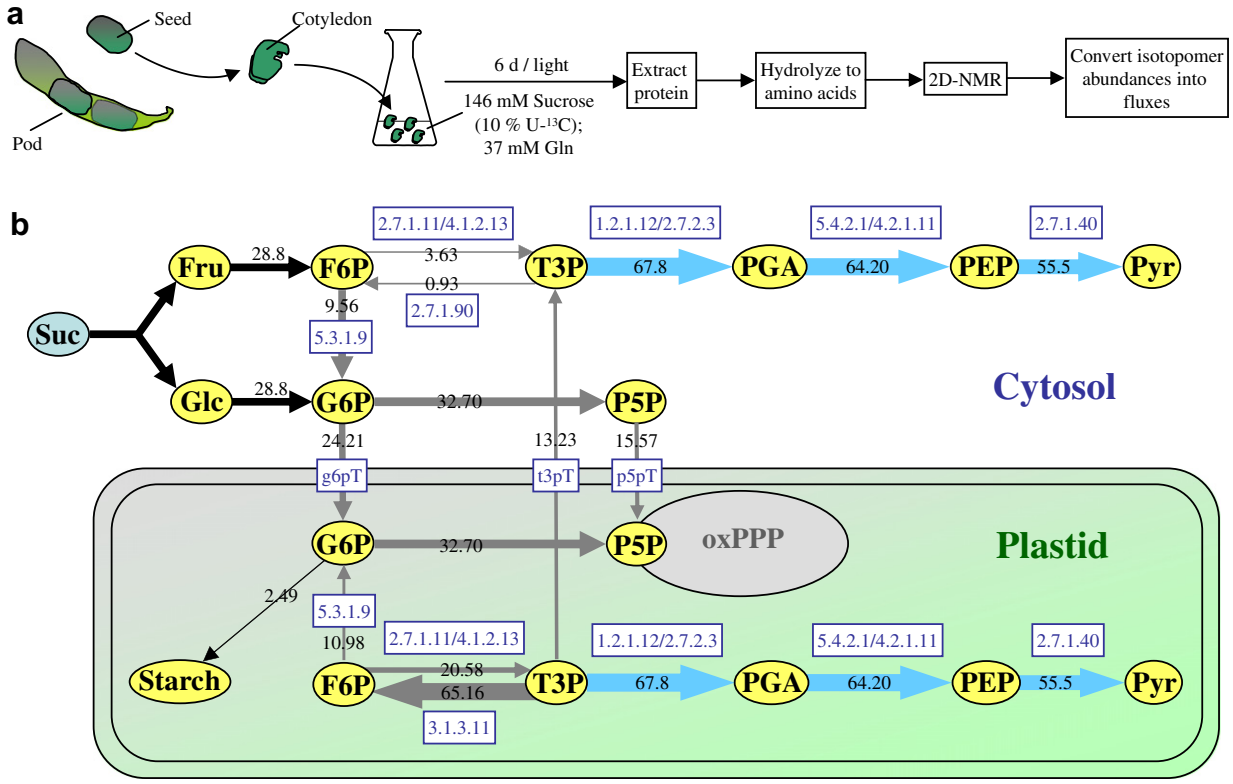

Fig. 2. Metabolic flux analysis of central carbon metabolism in developing soybean embryos (based upon data from Sriram et al., 2004). (a) Flowchart of pod harvest, embryo sampling, isotope feeding, protein extraction and processing, and data analysis. (b) Visualization of the control of glycolysis using the `BioPathAt` tool (Lange and Ghassemian, 2006). The widths of reaction arrows correlate with net fluxes. Net flux values are also given as μmol (day cotyledon)$^{-1}$. Enzymes are represented by their EC numbers. Black arrows indicate fluxes that are restricted to a particular subcellular compartment, gray arrows depict fluxes that occur in both the cytosol and plastids but can be distinguished, and light blue arrows indicate steps occurring in both compartments that cannot be distinguished based upon the data in Sriram et al. (2004). The values given in this figure are different from those published in the original paper; they are based upon a correction (www.plantphysiol.org/cgi/content/full/142/4/1771). (For interpretation of the references to color in this figure legend, the reader is referred to the web version of this article.)

ber in both the cytosol and plastids), whereas in other cases cytosolic and plastidial fluxes remained indistinguishable (light blue arrows in Fig. 2). Taken together the study by Sriram et al. (2004) represents the single most comprehensive metabolic flux analysis performed in a plant system to date. This integrative approach, which could be extended to other crop plants, has potential for providing valuable data to inform metabolic engineering and/or molecular breeding efforts aimed at enhancing key metabolic traits.

3. Kinetic analysis of metabolic networks

Stoichiometric network models can be generated using metabolic reconstructions that are based upon predictions of the coding capacity of sequenced genomes. This modeling approach is a first logical step in the exploration of the basic properties of the metabolic network. As outlined in Supplementary Material 1, linear programming tools can be used to calculate optimal flux distributions in the network when physicochemical constraints and objective functions (e.g., the systems is geared toward maximizing the yields of particular sink products) are applied. Methods of metabolic pathway analysis can then be used to obtain the feasible set of pathways operating in a given metabolic network. Isotopomer balancing can be employed to assign quantitative fluxes to specific branches of pathways or even individual steps. However, when scientists have aimed at changing fluxes by metabolic engineering (without disturbing the overall cell physiology), it has been very hard to determine the expression levels of which enzyme(s) needed to be modified. In complex networks (and almost all plant pathways have to be considered as being part of larger networks) intuitive approaches to the optimization of fluxes have remained unsatisfactory. Mathematical models that describe the dynamic properties of metabolic networks (predicting variation of metabolite concentrations over time) build on known rate equations (expressing enzyme properties and behavior in the presence of effectors) for individual enzymatic reactions and the definition of a metabolic network under consideration as a set of interdependent ODEs. Usually,algebraic solutions cannot be obtained for these systems of ODEs but various software packages have been introduced that allow calculating numerical solutions (iterative process of approximation and error correction) (for an overview of available software see Table 1). Once a kinetic model has been constructed it is possible to calculate the relative impact of an enzymatic step on the concentration of a metabolite the production of which one wishes to optimize. Although potentially very powerful and information-rich, such modeling efforts suffer from the disadvantage that most kinetic data are obtained with purified enzyme preparations in test tubes (*in vitro* kinetics), which might not be good reflections of kinetic characteristics within the cell (*in vivo* kinetics) (Steuer et al., 2006) and it has been suggested that approximative approaches to infer *in vivo* enzyme kinetics should be employed (Teusink et al., 2000; Heijnen, 2005).

3.1. Case study of kinetic modeling and dynamic simulation

We will consider the metabolic network described in Scheme 1 under the assumption that the transport fluxes $\boldsymbol{b}_1$, $\boldsymbol{b}_2$ and $\boldsymbol{b}_3$ exert negligible control over flux; this means that only the irreversible reaction fluxes $\boldsymbol{v}_1$, $\boldsymbol{v}_2$ and $\boldsymbol{v}_3$ need to be considered. To obtain the mass balances for metabolites $\boldsymbol{A}$, $\boldsymbol{B}$ and $\boldsymbol{C}$, the reaction network stoichiometry (I) is combined with Michaelis–Menten type enzyme kinetics (II) for each enzymatic step:

(I)Stoichiometric balances	(II)Michaelis–Menten rate equations
$\frac{dA}{dt} = -v_1 - v_2,$	$v_1 = v_{\max(Enz1)} \cdot \frac{A}{A + K_{m(Enz1)}},$
$\frac{dB}{dt} = v_1 - v_3,$	$v_3 = v_{\max(Enz3)} \cdot \frac{A}{A + K_{m(Enz3)}},$
$\frac{dC}{dt} = v_3 - v_2,$	$v_2 = v_{\max(Enz2)} \cdot \frac{A}{A + K_{m(Enz2)}}.$

The variation of metabolite concentration over time ($d\boldsymbol{M}/dt$) is equal to the difference of its rate of formation and its rate of consumption. Let us assume that we have measured an initial substrate concentration ($[A] = 1\ \mu M$) and that we have obtained the following values for K_m and V_{max} : $K_{m(Enz1)} = 0.8\ \mu M$; $K_{m(Enz2)} = 0.1\ \mu M$; $K_{m(Enz3)} = 0.004\ \mu M$; $V_{max(Enz1)} = 0.0018\ \mu M\ s^{-1}$; $V_{max(Enz2)} = 0.0018\ \mu M\ s^{-1}$; $V_{max(Enz3)} = 0.000012\ \mu M\ s^{-1}$. The simultaneous solution of the system of ODEs (for our example we used the 'ode45' function in the MATLAB® software; the code is available in Supplementary Material 1) then allows for the dynamic simulation of the changes in metabolite levels (Fig. 3).

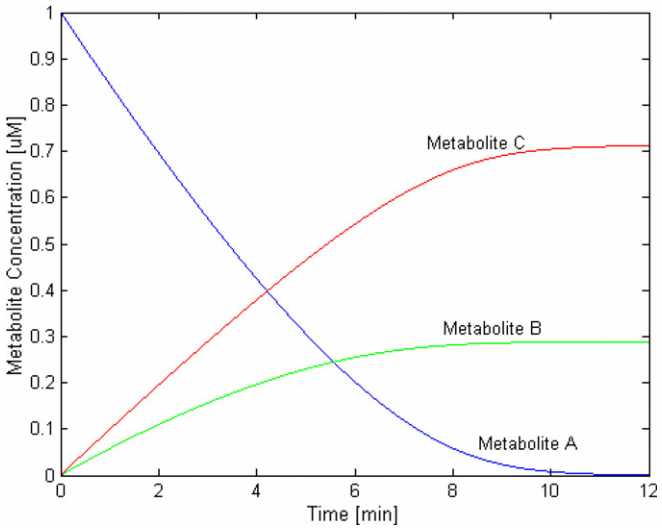

Fig. 3. Dynamic simulation of changes in metabolite concentrations over time for the metabolic network depicted in Scheme 1 (for assumed kinetic parameters and other details see text).

3.2. Kinetic models of plant metabolic networks

The majority of complex kinetic models generated to describe the control of plant metabolism are focused on photosynthesis and related pathways of central carbon metabolism (Table 2), which are among the most studied pathways in plants. Morgan and Rhodes (2002) have discussed the outcomes of these modeling efforts in an excellent recent review article. In this section we will thus not review these papers again but have decided to make a few comments about future directions. Most pathways of primary metabolism are somewhat conserved among eukaryotes and, if kinetic constants should not be available for a particular plant enzyme, they can be estimated based on the values obtained with the same enzyme from another organism. There is, of course, a danger when kinetic constants are inferred from the literature; thus, kinetic models need to be evaluated against experimental data. In this regard, measurements of metabolite pool sizes are of critical importance to test the performance of mathematical models. However, the quantification of pathway intermediates is analytically challenging and often neglected. Metabolite profiling efforts will need to emphasize increasing the spectrum of relevant metabolic intermediates (which usually do not accumulate at high levels and might be chemically unstable), so that an approximation of modeling and experimental results can be performed.

3.3. Metabolic control analysis

Metabolic control analysis (MCA) is a method for analyzing how control over fluxes and metabolite concentrations is distributed among the enzymes that constitute a metabolic pathway (or a network of pathways). Flux control is determined by applying experimental perturbations (one at a time) of each enzymatic step of interest (e.g., by over-expressing a particular enzyme in transgenic plants) and measuring the effect on the variable of interest after the system has reached a new steady-state. The magnitude of change in a network variable as a response to an experimental perturbation is expressed as a control coefficient such as the flux control coefficient (FCC):

$$C^{J}_{E_i} = \frac{\partial J/J}{\partial E_i/E_i} = \frac{\partial \ln J}{\partial \ln E_i},$$

where $C^{J}_{E_i}$ is the FCC of the ith enzyme, J is the steady-state flux, and E_i is the specific activity of ith enzyme.

According to the summation theorem, the sum of all FCCs in a metabolic network is equal to unity (Kacser and Burns, 1973; Heinrich and Rapoport, 1974; Giersch, 1988; Reder, 1988):

$$\sum_{i=1}^{n} C^{J}_{E_i} = 1 \quad \text{summation theorem},$$

where n corresponds to the number of enzymes involved in the metabolic system.

An important consequence of the summation theorem is that FCCs reflect global properties of a metabolic network; since control of flux is shared by all enzymes, the existence of rate-limiting steps is very unlikely. How does one actually assign FCCs? *In vitro* kinetic data that have been collected for the enzymes of a particular pathway can be used to calculate elasticity coefficients, which in turn can be used to calculate FCCs. Elasticity coefficients (ECs) establish a relationship between enzyme activity and its potential to control flux. The effect of a metabolite (***M***) on enzyme activity is quantified as the fractional change in the reaction rate (v) due to an infinitesimal change in the concentration of ***M*** (Fell, 1997):

$$\varepsilon^{E_i}_{M} \frac{\partial v_i/v_i}{\partial M/M} = \frac{\partial \ln v_i}{\partial \ln M}.$$

If ***M*** stimulates the rate of reaction (activator), $\varepsilon^{E_i}_{M}$ will be greater than zero; if ***M*** slows the reaction down (inhibitor), $\varepsilon^{E_i}_{M}$ will be negative. ECs are not systemic properties (unlike FCCs), but rather indicate how sensitive individual enzymes are to perturbations. The connectivity theorem of MCA states that the sum of the products of the FCCs and ECs of all (i) enzymatic steps affected by ***M*** equals zero:

$$\sum_{i=1}^{n} C^{J}_{E_i} \varepsilon^{E_i}_{M} = 0 \quad \text{Connectivity theorem},$$

where n is the total number of enzymes in the system.

In analogy to FCCs, MCA also defines coefficients that account for the effect of parameters such as enzyme activity on intracellular metabolite concentration; these are termed concentration control coefficients (CCCs). These coefficients specify the relative change in the level of the jth metabolite when the activity of the ith enzyme is changed (note that CCCs can have both positive and negative values):

$$C^{M_j}_{E_i} = \frac{E_i}{M_j} \cdot \frac{\partial M_j}{\partial E_i} = \frac{\partial \ln M_j}{\partial \ln E_i}.$$

The summation theorem also applies and states that the sum of all CCCs equals zero:

$$\sum_{i=1}^{n} C^{M_j}_{E_i} = 0.$$

MCA thus relates the kinetic properties of individual enzymes (local attributes) to the properties of the entire pathway or network of pathways (global attributes).

3.3.1. Case study of metabolic control analysis

Two different approaches can be used to determine FCCs. The indirect approach requires the determination of elasticities which, based upon the connectivity theorem, can be used to calculate FCCs. The direct experimental determination of FCCs involves the variation of enzyme activity and/or kinetic parameters (e.g., by overexpressing an enzyme using transgenic approaches or inhibitor titration) and quantifying changes under steady-state condi-

tions (Delgado and Liao, 1992) (Fig. 4). We will again use the example shown in Scheme 1 to illustrate the use of the direct approach. Let us assume that we have generated transgenic plants with varying levels of expression of the gene encoding ***Enz2*** (and thus varying levels of ***Enz2*** enzyme activity). By plotting enzyme activity versus flux as in Fig. 4, a hyperbolic curve is obtained (each 'x' symbolizes an enzyme activity/flux pair for one plant line). The graph represents the steady state pathway flux J as a function of the activity of an enzyme in the metabolic network under consideration. The calculation of the FCC for an enzyme at a specific enzyme activity ($\boldsymbol{E}^*$) is performed by taking the slope of the tangent at that enzyme activity $(\mathrm{d}J/\mathrm{d}E)|_{E=E^*}$ and multiplying it by a scaling factor. The scaling factor includes the enzyme activity normalized with respect to the steady state flux J^* : $\mathrm{FCC} = (\mathrm{d}J/\mathrm{d}E)|_{E=E^*} \cdot E/J = (\mathrm{d}J/J)/(\mathrm{d}E/E)$. The scaling process makes the FCCs dimensionless, reflecting rates of change in proportion to the enzyme activity and steady state flux, at the fixed point ($\boldsymbol{E}^*, \boldsymbol{J}^*$). In our example (Fig. 4), $\boldsymbol{E}^*$ for the wild-type plant is 6 (arbitrary units) and for the transgenic plant 16; $\boldsymbol{J}^*$ for wild-type plant is 0.5 (arbitrary units) and for the transgenic plant 0.75. The slope for the wild-type plant is 0.05 and for the transgenic plant 0.012. Thus, the FCCs for ***Enz2*** in the wild-type plants can be calculated as $0.05 \cdot 6/0.45 = 0.66$ and for the transgenic plant we obtain $0.012 \cdot 16/0.75 = 0.26$. Note that the FCC for ***Enz2*** in the transgenic plant overexpressing the gene encoding ***Enz2*** is actually lower than that for ***Enz2*** in the untransformed control plants, indicating that a 'bottleneck' created by ***Enz2*** in the control plant has been relieved in the transgenic plant. At the same time, the FCCs for all other enzymes in the transgenic plant will have changed as well and another enzyme might now be responsible for a 'bottleneck'. This example illustrates that an enzyme that might have been regarded as being rate-limiting using classical biochemical terms does not exert appreciable control over the pathway in the transgenic plant. Flux control is a dynamic process and all enzymes of a metabolic network contribute to it at varying degrees, which can change depending on the experimental conditions.

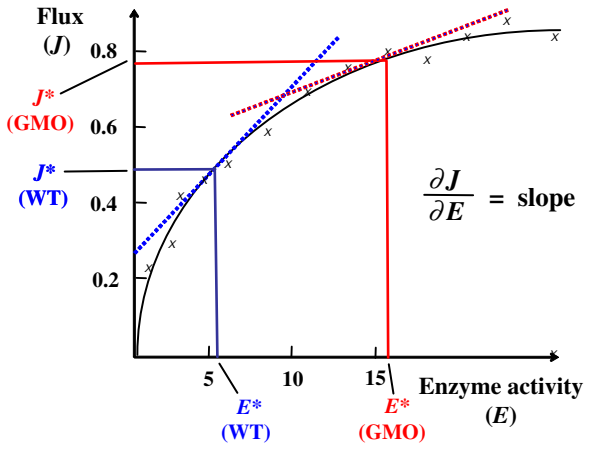

Fig. 4. Determination of flux control coefficients using the direct method of metabolic control analysis (for details see text). *Abbreviations*: GMO, transgenic plant; WT, wild-type plant.

3.3.2. Metabolic control analysis for modeling plant metabolic networks

3.3.2.1. Indirect metabolic control analysis. Poolman et al. (2000) introduced an approach to modeling photosynthetic pathways (in particular Calvin cycle, starch metabolism, and triose phosphate export) that distinguishes between two different steady-states depending on the magnitude of the carbon assimilatory flux. Based on an indirect MCA with regard to Calvin cycle enzymes, only sedoheptulose bisphosphatase (EC 3.1.3.37) and ribulose bisphosphate carboxylase/oxidase (Rubisco; EC 4.1.1.39) exert any significant control over assimilation. Once carbon is assimilated, other enzymes, most notably the triose phosphate transporter, become important in controlling the metabolic fate of assimilates. Thus, a simple strategy to increase carbon assimilation by transgenic over-expression of a small number of genes involved in the Calvin cycle is unlikely to be successful. Daae et al. (1999) used MCA to evaluate the feasibility of producing a polyhydroxyalkanoate polymer in transgenic plants. This analysis indicated that the adjustment of the ratio of the two precursor monomers would depend on growth conditions (light or dark), the expression levels of the four transgenes, and the availability of enzyme cofactors. For the development of a commercial production system, all of these variables would have to be carefully considered and controlled. Curien et al. (2003) developed a kinetic model around phosphohomoserine, an intermediate metabolite at the branchpoint of methionine and threonine biosynthesis. The authors also considered that, based on *in vitro* assays, flux is regulated by various allosteric controls. An iterative approach of mathematical modeling and *in vitro* experimentation was then employed to develop a model that can be used to interrogate which changes in methionine and threonine levels are to be expected when the amounts of specific components of the metabolic network are modulated. The role of redistribution of flux control in the competing branches of glutathione (GSH) and phytochelatin metabolism under Cadmium stress conditions was studied by Mendoza-Cózatl and Moreno-Sánchez (2006). In unstressed plants GSH levels are controlled by demand, whereas under Cadmium stress various enzymes control the accumulation levels of GSH and phytochelatins. Transgenic approaches to increase phytochelatin amounts (and thus Cadmium tolerance) without affecting GSH levels would need to take into account that a balance between competing pathways needs to be maintained.

3.3.2.2. Direct metabolic control analysis. Kruckeberg et al. (1989) evaluated the significance of plastidial and cytosolic isoforms of phosphoglucose isomerase (EC 5.3.1.9) in controlling the synthesis of starch and sucrose using a direct MCA approach based on results obtained with

decreased-activity mutants. The plastidial isozyme was found to exert considerable control over starch biosynthesis only under high light and CO_2 conditions, whereas the cytosolic isozyme exerted appreciable control only in the dark. The primary role of the cytosolic isozyme appeared to be its involvement in sucrose synthesis. Direct MCA to estimate control coefficients for an individual enzyme in transgenic plants with varying expression (and thus specific activity) levels was also performed for Rubisco in tobacco plants (Quick et al., 1991; Stitt et al., 1991) the glycolysis enzyme phosphofructokinase (EC 2.7.1.11) in potato tubers (Thomas et al., 1997a,b) the gluconeogenic enzyme isocitrate lyase (EC 4.1.3.1) in castor bean seedling endosperm (Runquist and Kruger, 1999) the carotenogenic enzyme phytoene synthase (EC 2.5.1.32) in tomato fruits (Fraser et al., 2002), and the lipid biosynthetic enzyme diacylglycerol acyltransferase (EC 2.3.1.20) in olive and oil palm tissue cultures (Ramli et al., 2005). Inhibitor titration studies allowed direct MCA to be employed for evaluating the importance of acetyl coenzyme A carboxylase (EC 6.4.1.2) in regulating lipid biosynthesis (Page et al., 1994), for determining the control of ammonia assimilation in isolated barley chloroplasts (Baron et al., 1994), and for investigating respiratory flux in isolated turnip mitochondria (Padovan et al., 1989). The outcomes of these direct MCA studies have been covered in previous reviews (Morgan and Rhodes, 2002; Fernie et al., 2005) and will not be discussed in detail here.

3.3.2.3. Top down control analysis. If kinetic information is not available for all enzymes in a metabolic pathway (or a more complex network of pathways), the application of 'top down' control analysis (TDCA), an MCA approach that groups several reactions in 'black boxes' around key intermediates, may provide useful information (Brown et al., 1990). TDCA was successfully employed to examine the relative importance of two blocks of lipid biosynthesis (plastidial fatty acid biosynthesis and lipid assembly in the cytosol) in olive and oil palm callus cultures (Ramli et al., 2002). Although the biosynthesis block exerted higher control than the lipid assembly block, both blocks exert significant control; thus, an over-expression of a single enzyme (or even a small set of enzymes) in transgenic olive or oil palm cultures is unlikely to result in increased oil yield. In general, all of the above-mentioned MCA studies have confirmed that the presence of a true rate-limiting enzyme is an extremely rare case.

3.3.2.4. Highlight: carotenoid biosynthesis in tomato fruits. We will discuss one recent paper in more detail as an example to illustrate this fact (Fraser et al., 2002). The roots of this project go back to the early 1990s, when attempts to increase carotenoid content in transgenic tomato plants by over-expressing a constitutive copy of the carotenoid biosynthetic enzyme phytoene synthase (PSY; EC 2.5.1.32) were frustrated by ectopic pigment production and a stunted growth phenotype (Fray and Grierson, 1993). Follow-up work established that dwarfism was caused by a lack of precursor availability for the biosynthesis of gibberellins (Fray et al., 1995), which, like carotenoids, are derived from geranylgeranyl diphosphate as an intermediate (Fig. 5). Fraser et al. (2002) employed constructs featuring a fruit-specific promoter and a transit sequence, thus targeting recombinant PSY protein to chromoplasts of tomato fruits. The FCC of PSY was determined to be 0.36, whereas FCCs for other enzymes considered

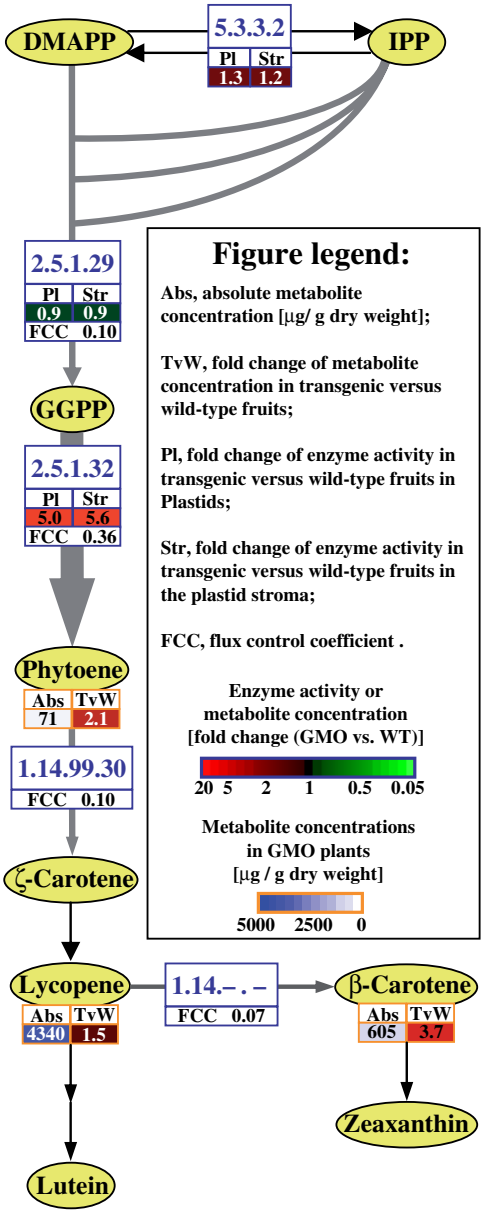

Fig. 5. Metabolic control analysis of carotenoid biosynthesis in tomato fruits (based upon data from Fraser et al., 2002). The `BioPathAt` tool was used to visualize (color-coded) ratios of enzyme activities and metabolite concentrations (transgenic versus wild-type plants) and absolute metabolite concentrations. Enzymes are represented by their EC numbers. The widths of reaction arrows correlate with flux control coefficients. *Abbreviations for metabolites*: DMAPP, dimethylallyl diphosphate; GGPP, geranylgeranyl diphosphate; IPP, isopentenyl diphosphate.

were at 0.1 or lower (Fig. 5). The 5–10-fold over-expression of PSY (at the level of specific enzyme activity) lead only to a roughly two-fold increase in total carotenoids. The FCC decreased from 0.36 (wild-type controls) to 0.15 (transgenic plants) with only very moderate increases in carotenoid content, indicating that flux control is shared by several enzymes in the carotenoid pathway.

4. Conclusions

Various innovative approaches for metabolic flux analysis have been employed with plants in recent years (e.g., elementary modes analysis and isotopomer balancing), with other methods having potential although they have not yet been utilized (e.g., extreme pathway analysis). Metabolic flux analysis is a very active research field and has yielded valuable insights particularly into the regulation of central carbon metabolism. In contrast, kinetic approaches to estimate flux control were pursued by numerous groups in the 1990s and early 2000s but only a few studies have been published in this area recently. This might in part be due to a shift in governmental funding priorities, which have led to vast increases in the number of genomics-based studies, whereas our knowledge regarding the kinetic properties of individual metabolic enzymes has not kept pace. Both approaches depend on each other to provide an in-depth understanding of flux control and it should thus be a high priority for funding agencies to help reinvigorate classical biochemistry.

Acknowledgments

R.R.E. thanks the Fulbright Program and the University of Antioquia for scholarships; B.M.L. thanks the National Science Foundation (award 0520140) and the Agricultural Research Center at Washington State University for funding. The authors also thank Dr. W. Wiechert (University of Siegen, Germany) for advice on the section describing the isotopomer approach to flux analysis. We also thank two anonymous reviewers for valuable comments that have considerably improved this manuscript.

Appendix A. Supplementary data

Supplementary data associated with this article can be found, in the online version, at doi:10.1016/j.phytochem.2007.04.021.

References

Alves, R., Antunes, F., Salvador, A., 2006. Tools for kinetic modeling of biochemical networks. Nature Biotechnology 24, 667–672.

Alonso, A.P., Vigeolas, H., Raymond, P., Rolin, D., Dieuaide-Noubhani, M., 2006. A new substrate cycle in plants. Evidence for a high glucose-phosphate-to-glucose turnover from in vivo steady-state and pulse-labeling experiments with [^{13}C]glucose and [^{14}C]glucose. Plant Physiology 138, 2220–2232.

Antoniewicz, M.R., Kelleher, J.K., Stephanopoulos, G., 2007. Elementary metabolite units (EMU): a novel framework for modeling isotopic distributions. Metabolic Engineering 9, 68–86.

Baron, A.C., Tobin, T.H., Wallsgrove, R.M., Tobin, A.K., 1994. A metabolic control analysis of the glutamine synthetase/glutamate synthase cycle in isolated barley (*Hordeum vulgare* L.) chloroplasts. Plant Physiology 105, 415–424.

Bell, S.L., Palsson, B.Ø., 2005. `Expa`: a program for calculating extreme pathways in biochemical reaction networks. Bioinformatics 21, 1739–1740.

Blasius, B., Beck, F., Lüttge, U., 1997. A model for photosynthetic oscillations in Crassulacean acid metabolism (CAM). Journal of Theoretical Biology 184, 345–351.

Blasius, B., Beck, F., Lüttge, U., 1998. Oscillatory model of Crassulacean acid metabolism: structural analysis and stability boundaries with a discrete hysteresis switch. Plant, Cell and Environment 21, 775–784.

Blasius, B., Neff, R., Beck, F., Lüttge, U., 1999. Oscillatory model of Crassulacean acid metabolism with dynamic hysteresis switch. Proceedings of the Royal Society of London B: Biological Sciences 266, 93–101.

Boatright, J., Negre, F., Chen, X., Kish, C.M., Wood, B., Peel, G., Orlova, I., Gang, D., Rhodes, D., Dudareva, N., 2004. Understanding in vivo benzenoid metabolism in petunia petal tissue. Plant Physiology 135, 1993–2011.

Brown, G.C., Hafner, R.P., Brand, M.D., 1990. A 'top-down' approach to the determination of control coefficients in metabolic control theory. European Journal of Biochemistry 188, 321–325.

Caiveau, O., Fortune, D., Cantrel, C., Zachowski, A., Moreau, F., 2001. Consequences of omega-6-oleate desaturase deficiency on lipid dynamics and functional properties of mitochondrial membranes of *Arabidopsis thaliana*. Journal of Biological Chemistry 276, 5788–5794.

Chen, D.X., Coughenour, M.B., Knapp, A.K., Owensby, C.E., 1994. Mathematical simulation of C4 grass photosynthesis in ambient and elevated CO_2. Ecological Modelling 73, 63–80.

Collatz, G.J., Ribas-Carbo, M., Berry, J.A., 1992. Coupled photosynthesis-stomatal conductance model for leaves of C4 plants. Australian Journal of Plant Physiology 19, 519–538.

Curien, G., Ravanel, S., Dumas, R., 2003. A kinetic model of the branch-point between the methionine and threonine biosynthesis pathways in *Arabidopsis thaliana*. European Journal of Biochemistry 270, 4615–4627.

Daae, E.B., Dunnill, P., Mitsky, T.A., Padgette, S.R., Taylor, N.B., Valentin, H.E., Gruys, K.J., 1999. Metabolic modeling as a tool for evaluating polyhydroxyalkanoate copolymer production in plants. Metabolic Engineering 1, 243–254.

Delgado, J., Liao, J.C., 1992. Determination of flux control coefficients from transient metabolite concentrations. Biochemical Journal 282, 919–927.

DellaPenna, D., 2001. Plant metabolic engineering. Plant Physiology 125, 160–163.

Dhar, P., Meng, T.C., Somani, S., Ye, L., Sairam, A., Chitre, M., Hao, Z., Sakharkar, K., 2004. Cellware – a multi-algorithmic software for computational systems biology. Bioinformatics 20, 1319–1321.

Dieuaide-Noubhani, M., Raffard, G., Canioni, P., Pradet, A., Raymond, P., 1995. Quantification of compartmented metabolic fluxes in maize root tips using isotope distribution from ^{13}C- or ^{14}C-labeled glucose. Journal of Biological Chemistry 270, 13147–13159.

Edwards, S., Nguyen, B.T., Do, B., Roberts, J.K.M., 1998. Contribution of malic enzyme, pyruvate kinase, phosphoenolpyruvate carboxylase, and the Krebs cycle to respiration and biosynthesis and to intracellular pH regulation during hypoxia in maize root tips observed by nuclear magnetic resonance imaging and gas chromatography-mass spectrometry. Plant Physiology 116, 1073–1081.

Ettenhuber, C., Radykewicz, T., Kofer, W., Koop, H.U., Bacher, A., Eisenreich, W., 2005a. Metabolic flux analysis in complex isotopolog

space. Recycling of glucose in tobacco plants. Phytochemistry 66, 323–335.

Ettenhuber, C., Spielbauer, G., Margl, L., Hannah, L.C., Gierl, A., Bacher, A., Genschel, U., Eisenreich, W., 2005b. Changes in flux pattern of the central carbohydrate metabolism during kernel development in maize. Phytochemistry 66, 2632–2642.

Farquhar, G.D., von Caemmerer, C., Berry, J.A., 1980. A biochemical model of photosynthetic CO_2 assimilation in leaves of C_3 species. Planta 149, 78–90.

Fell, D.A., 1997. Understanding the Control of Metabolism. Portland Press, London, UK.

Fernie, A.R., Roscher, A., Ratcliffe, R.G., Kruger, N.J., 2001. Fructose 2,6-bisphosphate activates pyrophosphate: fructose-6-phosphate 1-phosphotransferase and increases triose phosphate to hexose phosphate cycling in heterotrophic cells. Planta 212, 250–263.

Fernie, A.R., Geigenberger, P., Stitt, M., 2005. Flux an important, but neglected, component of functional genomics. Current Opinion in Plant Biology 8, 174–182.

Fraser, P.D., Romer, S., Shipton, C.A., Mills, P.B., Kiano, J.W., Misawa, N., Drake, R.G., Schuch, W., Bramley, P.M., 2002. Evaluation of transgenic tomato plants expressing an additional phytoene synthase in a fruit-specific manner. Proceedings of the National Academy of Sciences of the United States of America 99, 1092–1097.

Fray, R.G., Grierson, D., 1993. Identification and genetic analysis of normal and mutant phytoene synthase genes of tomato by sequencing, complementation and co-suppression. Plant and Molecular Biology 22, 589–602.

Fray, R.G., Wallace, A., Fraser, P.D., Valero, D., Hedden, P., Bramley, P.M., Grieson, D., 1995. Constitutive expression of a fruit phytoene synthase gene in transgenic tomatoes causes dwarfism by redirecting metabolites from the gibberellin pathway. The Plant Journal 8, 693–701.

Fridlyand, L.E., 1998. Independent changes of ATP/ADP or Delta-pH could cause oscillations in photosynthesis. Journal of Theoretical Biology 193, 739–741.

Fridlyand, L.E., Backhausen, J.E., Scheibe, R., 1998. Flux control of the malate valve in leaf cells. Archives of Biochemistry and Biophysics 349, 290–298.

Fridlyand, L.E., Scheibe, R., 1999. Regulation of the Calvin cycle for CO_2 fixation as an example for general control mechanisms in metabolic cycles. Biosystems 51, 79–93.

Fridlyand, L.E., Scheibe, R., 2000. Regulation in metabolic systems under homeostatic flux control. Archives of Biochemistry and Biophysics 374, 198–206.

Funahashi, A., Tanimura, N., Morohashi, M., Kitano, H., 2003. CellDesigner: a process diagram editor for gene-regulatory and biochemical networks. Biosilico 1, 159–162.

Gagneur, J., Klamt, S., 2004. Computation of elementary modes: a unifying framework and the new binary approach. BMC Bioinformatics 5, 175.

Giersch, C., 1988. Control analysis of biochemical pathways: a novel procedure for calculating control coefficients, and an additional theorem for branched pathways. Journal of Theoretical Biology 134, 451–462.

Giersch, C., 2000. Mathematical modelling of metabolism. Current Opinion in Plant Biology 3, 249–253.

Glawischnig, E., Gierl, A., Tomas, A., Bacher, A., Eisenreich, W., 2001. Retrobiosynthetic nuclear magnetic resonance analysis of amino acid biosynthesis and intermediary metabolism. Metabolic flux in developing maize kernels. Plant Physiology 125, 1178–1186.

Glawischnig, E., Gierl, A., Tomas, A., Bacher, A., Eisenreich, W., 2002. Starch biosynthesis and intermediary metabolism in maize kernels. Quantitative analysis of metabolite flux by nuclear magnetic resonance. Plant Physiology 130, 1717–1727.

Gross, L.J., Kirschbaum, M., Pearcy, R.W., 1991. A dynamic model of photosynthesis in varying light taking account of stomatal conductance, C[3]-cycle intermediates, photorespiration and Rubisco activation. Plant, Cell and Environment 14, 881–893.

He, D., Edwards, G.E., 1996. Estimation of diffusive resistance of bundle sheath cells to CO_2 from modeling of C_4 photosynthesis. Photosynthesis Research 49, 195–208.

Heinrich, R., Rapoport, T.A., 1974. A linear steady-state treatment of enzymatic chains. General properties, control and effector strength. European Journal of Biochemistry 42, 89–95.

Heinrich, R., Schuster, S., 1996. The Regulation of Cellular Systems. Chapman & Hall, New York.

Heijnen, J.J., 2005. Approximative kinetic formats used in metabolic network modeling. Biotechnology and Bioengineering 91, 534–545.

Hoops, S., Sahle, S., Gauges, R., Lee, C., Pahle, J., Simus, N., Singhal, M., Xu, L., Mendes, P., Kummer, U., 2006. COPASI – a COmplex PAthway SImulator. Bioinformatics 22, 3067–3074.

Jeffrey, F.M.H., Rajagopal, A., Malloy, C.R., Sherry, A.D., 1991. ^{13}C NMR: a simple yet comprehensive method for analysis of intermediary metabolism. Trends in Biochemical Sciences 16, 5–10.

Kacser, H., Burns, J.A., 1973. The control of flux. Symposium of the Society of Experimental Biology 27, 65–104.

Kirschbaum, M.U.F., 1994. The sensitivity of C[3] photosynthesis to increasing CO[2] concentration: a theoretical analysis of its dependence on temperature and background CO[2] concentration. Plant, Cell and Environment 17, 747–754.

Kirschbaum, M.U.F., Küppers, M., Schneider, H., Giersch, C., Noe, S., 1997. Modelling photosynthesis in fluctuating light with inclusion of stomatal conductance, biochemical activation and pools of key photosynthetic intermediates. Planta 204, 16–26.

Klamt, S., Stelling, J., 2003. Two approaches for metabolic pathway analysis? Trends in Biotechnology 21, 64–69.

Klamt, S., Stelling, J., Ginkel, M., Gilles, E.D., 2003. `FluxAnalyzer`: exploring structure, pathways, and flux distributions in metabolic networks on interactive flux maps. Bioinformatics 19, 261–269.

Krab, K., 1995. Kinetic and regulatory aspects of the function of the alternative oxidase in plant respiration. Journal of Bioengineering and Biomembranes 27, 387–396.

Kruckeberg, A.L., Neuhaus, H.E., Feil, R., Gottlieb, L.D., Stitt, M., 1989. Decreased-activity mutants of phosphoglucose isomerase in the cytosol and chloroplast of *Clarkia xantiana*. Impact on mass-action ratios and fluxes to sucrose and starch, and estimation of flux control coefficients and elasticity coefficients. Biochemical Journal 261, 457–467.

Laisk, A., Edwards, G.E., 2000. A mathematical model of C(4) photosynthesis: the mechanism of concentrating CO(2) in NADP-malic enzyme type species. Photosynthesis Research 66, 199–224.

Lange, B.M., 2006. Integrative analysis of metabolic networks: from peaks to flux models? Current Opinion in Plant Biology 9, 220–226.

Lange, B.M., Ghassemian, M., 2006. Comprehensive post-genomic data analysis approaches integrating biochemical pathway maps. Phytochemistry 66, 413–451.

Latowski, D., Burda, K., Strzalka, K., 2000. A mathematical model describing kinetics of conversion of violaxanthin to zeaxanthin via intermediate antheraxanthin by the xanthophyll cycle enzyme violaxanthin de-epoxidase. Journal of Theoretical Biology 206, 507–514.

Leduc, M., Tikhomiroff, C., Cloutier, M., Perrier, M., Jolicoeur, M., 2006. Development of a kinetic metabolic model: application to *Catharanthus roseus* hairy root. Bioprocess and Biosystems Engineering 28, 295–313.

Lee, D.Y., Yun, C., Cho, A., Hou, B.K., Park, S., Lee, S.Y., 2006. WebCell: a web-based environment for kinetic modeling and dynamic simulation of cellular networks. Bioinformatics 22, 1150–1151.

Le Novere, N., Finney, A., Hucka, M., Bhalla, U.S., Campagne, F., Collado-Vides, J., Crampin, E.J., Halstead, M., Klipp, E., Mendes, P., Nielsen, P., Sauro, H., Shapiro, B., Snoep, J.L., Spence, H.D., Wanner, B.L., 2005. Minimum information requested in the annotation of biochemical models (MIRIAM). Nature Biotechnology 23, 1509–1515.

Le Novere, N., Bornstein, B., Broicher, A., Courtot, M., Donizelli, M., Dharuri, H., Li, L., Sauro, H., Schilstra, M., Shapiro, B., Snoep, J.L., Hucka, M., 2006. BioModels Database: a free, centralized database of curated, published, quantitative kinetic models of biochemical and cellular systems. Nucleic Acids Research 34, D689–D691.

Malone, J.G., Mittova, V., Ratcliffe, R.G., Kruger, N.J., 2006. The response of carbohydrate metabolism in potato tubers to low temperature. Plant and Cell Physiology 47, 1309–1322.

Martinez-Force, E., Garces, R., 2000. Metabolic control analysis of *de novo* sunflower fatty acid biosynthesis. Biochemical Society Transactions 28, 669–671.

Matsuda, F., Morino, K., Miyashita, M., Miyagawa, H., 2003. Metabolic flux analysis of the phenylpropanoid pathway in wound-healing potato tuber tissue using stable isotope-labeled tracer and LC-MS spectroscopy. Plant and Cell Physiology 44, 510–517.

Matsuda, F., Morino, K., Ano, R., Kuzawa, M., Wakasa, K., Miyagawa, H., 2005. Metabolic flux analysis of the phenylpropanoid pathway in elicitor-treated potato tuber tissue. Plant and Cell Physiology 46, 454–466.

McNeil, S.D., Nuccio, M.L., Rhodes, D., Shachar-Hill, Y., Hanson, A.D., 2000a. Radiotracer and computer modeling evidence that phosphobase methylation is the main route of choline synthesis in tobacco. Plant Physiology 123, 371–380.

McNeil, S.D., Rhodes, D., Russell, B.L., Nuccio, M.L., Shachar-Hill, Y., Hanson, A.D., 2000b. Metabolic modeling identifies key constraints on an engineered glycine betaine synthesis pathway in tobacco. Plant Physiology 124, 153–162.

Mendes, P., 1993. GEPASI: a software package for modelling the dynamics, steady states and control of biochemical and other systems. Computer Applications in the Biosciences 9, 563–571.

Mendoza-Cózatl, D.G., Moreno-Sánchez, R., 2006. Control of glutathione and phytochelatin synthesis under cadmium stress. Pathway modeling for plants. Journal of Theoretical Biology 238, 919–936.

Morgan, J.A., Rhodes, D., 2002. Mathematical modeling of plant metabolic pathways. Metabolic Engineering 4, 80–89.

Neff, R., Blasius, B., Beck, F., Lüttge, U., 1998. Thermodynamics and energetics of the tonoplast membrane operating as a hysteresis switch in an oscillatory model of Crassulacean acid metabolism. Journal of Membrane Biology 165, 37–43.

Nuccio, M.L., McNeil, S.D., Ziemak, M.J., Hanson, A.D., Jain, R.K., Selvaraj, G., 2000. Choline import into chloroplasts limits glycine betaine synthesis in tobacco: analysis of plants engineered with a chloroplastic or a cytosolic pathway. Metabolic Engineering 2, 300–311.

Nungesser, D., Kluge, M., Tolle, H., Oppelt, W., 1984. A dynamic computer model of the metabolic and regulatory processes in Crassulacean acid metabolism. Planta 162, 204–214.

Olivier, B.G., Snoep, J.L., 2004. Web-based kinetic modelling using JWS Online. Bioinformatics 20, 2143–2144.

Padovan, A.C., Dry, I.B., Wiskich, J.T., 1989. An analysis of the control of phosphorylation-coupled respiration in isolated plant mitochondria. Plant Physiology 90, 928–933.

Page, R.A., Okada, S., Harwood, J.L., 1994. Acetyl-CoA carboxylase exerts strong flux control over lipid biosynthesis in plants. Biochimica et Biophysica Acta 1210, 369–372.

Papin, J.A., Price, N.D., Palsson, B.Ø., 2002. Extreme pathway lengths and reaction participation in genome-scale metabolic networks. Genome Research 12, 1889–1900.

Pearcy, R.W., Gross, L.J., He, D., 1997. An improved dynamic model of photosynthesis for estimation of carbon gain in sunfleck light regimes. Plant, Cell and Environment 20, 411–424.

Pettersson, G., 1997. Control properties of the Calvin photosynthesis cycle at physiological carbon dioxide concentrations. Biochimica et Biophysica Acta 1322, 173–182.

Pettersson, G., Ryde-Pettersson, U., 1988. A mathematical model of the Calvin photosynthesis cycle. European Journal of Biochemistry 175, 661–672.

Polle, A., 2001. Dissecting the superoxide dismutase-ascorbate-glutathione-pathway in chloroplasts by metabolic modeling. Computer simulations as a step towards flux analysis. Plant Physiology 126, 445–462.

Poolman, M.G., Fell, D.A., Thomas, S., 2000. Modelling photosynthesis and its control. Journal of Experimental Botany 51, 319–328.

Poolman, M.G., Fell, D.A., Raines, C.A., 2003. Elementary modes analysis of photosynthate metabolism in the chloroplast stroma. European Journal of Biochemistry 270, 430–439.

Price, N.D., Reed, J.L., Papin, J.A., Famili, I., Palsson, B.Ø., 2003. Analysis of metabolic capabilities using singular value decomposition of extreme pathway matrices. Biophysical Journal 84, 794–804.

Price, N.D., Reed, J.L., Palsson, B.Ø., 2004. Genome-scale models of microbial cells: evaluating the consequences of constraints. Nature Reviews in Microbiology 2, 886–897.

Quick, W.P., Schurr, U., Scheibe, R., Schulze, E.D., Rodermel, S.R., Bogorad, L., Stitt, M., 1991. Decreased ribulose-1,5-bisphosphate carboxylase-oxygenase in transgenic tobacco transformed with "antisense" rbcS. 1. Impact on photosynthesis in ambient growth conditions. Planta 183, 542–554.

Ramli, U.S., Salas, J.J., Quant, P.A., Harwood, J.L., 2002. Control analysis of lipid biosynthesis in tissue cultures from oil crops shows that flux control is shared between fatty acid synthesis and lipid assembly. Biochemical Journal 364, 393–401.

Ramli, U.S., Salas, J.J., Quant, P.A., Harwood, J.L., 2005. Metabolic control analysis reveals an important role for diacylglycerol acyltransferase in olive but not in oil palm lipid accumulation. FEBS Journal 272, 5764–5770.

Ramsey, S., Orrell, D., Bolouri, H., 2005. Dizzy: stochastic simulation of large-scale genetic regulatory networks. Journal of Bioinformatics and Computational Biology 3, 415–436.

Ratcliffe, R.G., Shachar-Hill, Y., 2001. Probing plant metabolism with NMR. Annual Review of Plant Physiology and Plant Molecular Biology 52, 499–526.

Ratcliffe, R.G., Shachar-Hill, Y., 2006. Measuring multiple fluxes through plant metabolic networks. The Plant Journal 45, 490–511.

Reder, C., 1988. Metabolic control theory: a structural approach. Journal of Theoretical Biology 135, 175–201.

Roessner-Tunali, U., Liu, J., Leisse, A., Balbo, I., Perez-Melis, A., Willmitzer, L., Fernie, A.R., 2004. Kinetics of labelling of organic and amino acids in potato tubers by gas chromatography-mass spectrometry following incubation in (13)C labelled isotopes. The Plant Journal 39, 668–679.

Rohwer, J.M., Botha, F.C., 2001. Analysis of sucrose accumulation in the sugar cane culm on the basis of in vitro kinetic data. Biochemical Journal 358, 437–445.

Rontein, D., Dieuaide-Noubhani, M., Dufourc, E.J., Raymond, P., Rolin, D., 2002. The metabolic architecture of plant cells. Stability of central metabolism and flexibility of anabolic pathways during the growth cycle of tomato cells. Journal of Biological Chemistry 277, 43948–43960.

Roscher, A., Emsley, L., Raymond, P., Roby, C., 1998. Unidirectional steady state rates of central metabolism enzymes measured simultaneously in a living plant tissue. Journal of Biological Chemistry 273, 25053–25061.

Roscher, A., Kruger, N.J., Ratcliffe, R.G., 2000. Strategies for metabolic flux analysis in plants using isotope labelling. Journal of Biotechnology 77, 81–102.

Runquist, M., Kruger, N.J., 1999. Control of gluconeogenesis by isocitrate lyase in endosperm of germinating castor bean seedlings. The Plant Journal 19, 423–431.

SBML Forum, 2003. The systems biology markup language (SBML): a medium for representation and exchange of biochemical network models. Bioinformatics 19, 524–531.

Schilling, C.H., Edwards, J.S., Palsson, B.Ø., 1999. Toward metabolic phenomics: analysis of genomic data using flux balances. Biotechnology Progress 15, 288–295.

Schilling, C.H., Letscher, D., Palsson, B.Ø., 2000. Theory for the systemic definition of metabolic pathways and their use in interpreting metabolic function from a pathway-oriented perspective. Journal of Theoretical Biology 203, 229–248.

Schilling, C.H., Edwards, J.S., Letscher, D., Palsson, B.Ø., 2001. Combining pathway analysis with flux balance analysis for the comprehensive study of metabolic systems. Biotechnology and Bioengineering 71, 286–306.

Schmidt, K., Carlsen, M., Nielsen, J., Villadsen, J., 1997. Modeling isotopomer distributions in biochemical networks using isotopomer mapping matrices. Biotechnology and Bioengineering 55, 831–840.

Schmidt, K., Norregaard, L.C., Pedersen, B., Meissner, A., Duus, J.O., Nielsen, J.O., Villadsen, J., 1999. Quantification of intracellular metabolic fluxes from fractional enrichment and ^{13}C–^{13}C coupling constraints on the isotopomer distribution in labeled biomass components. Metabolic Engineering 1, 166–179.

Schmidt, H., Jirstrand, M., 2006. Systems Biology Toolbox for MATLAB: a computational platform for research in systems biology. Bioinformatics 22, 514–515.

Schuster, S., Hilgetag, C., 1994. On elementary flux modes in biochemical reaction systems at steady state. Journal of Biological Systems 2, 165–182.

Schuster, S., Dandekar, T., Fell, D.A., 1999. Detection of elementary flux modes in biochemical networks: a promising tool for pathway analysis and metabolic engineering. Trends in Biotechnology 17, 53–60.

Schwarz, R., Musch, P., von Kamp, A., Engels, B., Schirmer, H., Schuster, S., Dandekar, T., 2005. YANA – a software tool for analyzing flux modes, gene-expression and enzyme activities. BMC Bioinformatics 6, 135.

Schwender, J., Ohlrogge, J.B., 2002. Probing in vivo metabolism by stable isotope labeling of storage lipids and proteins in developing *Brassica napus* embryos. Plant Physiology 130, 347–361.

Schwender, J., Ohlrogge, J.B., Shachar-Hill, Y., 2003. A flux model of glycolysis and the oxidative pentosephosphate pathway in developing *Brassica napus* embryos. Journal of Biological Chemistry 278, 29442–29453.

Schwender, J., Ohlrogge, J., Shachar-Hill, Y., 2004a. Understanding flux in plant metabolic networks. Current Opinion in Plant Biology 7, 309–317.

Schwender, J., Goffman, F., Ohlrogge, J.B., Shachar-Hill, Y., 2004b. Rubisco without the Calvin cycle improves the carbon efficiency of developing green seeds. Nature 432, 779–782.

Schwender, J., Shachar-Hill, Y., Ohlrogge, J.B., 2006. Mitochondrial metabolism in developing embryos of *Brassica napus*. Journal of Biological Chemistry 281, 34040–34047.

Selivanov, V.A., Marin, S., Lee, P.W., Cascante, M., 2006. Software for dynamic analysis of tracer-based metabolomic data: estimation of metabolic fluxes and their statistical analysis. Bioinformatics 22, 2806–2812.

Sielewiesiuk, J., Gruszecki, W.I., 1991. A simple model describing the kinetics of the xanthophyll cycle. Biophysical Chemistry 41, 125–129.

Slater, S., Mitsky, T.A., Houmiel, K.L., Hao, M., Reiser, S.E., Taylor, N.B., Tran, M., Valentin, H.E., Rodriguez, D.J., Stone, D.A., Padgette, S.R., Kishore, G., Gruys, K.J., 1999. Metabolic engineering of *Arabidopsis* and *Brassica* for poly(3-hydroxybutyrate-*co*-3-hydroxyvalerate) copolymer production. Nature Biotechnology 17, 1011–1016.

Spielbauer, G., Margl, L., Hannah, L.C., Romisch, W., Ettenhuber, C., Bacher, A., Gierl, A., Eisenreich, W., Genschel, U., 2006. Robustness of central carbohydrate metabolism in developing maize kernels. Phytochemistry 67, 1460–1475.

Sriram, G., Shanks, J.V., 2004. Improvements in metabolic flux analysis using carbon bond labeling experiments: bondomer balancing and Boolean function mapping. Metabolic Engineering 6, 116–132.

Sriram, G., Fulton, D.B., Iyer, V.V., Peterson, J.M., Zhou, R., Westgate, M.E., Spalding, M.H., Shanks, J.V., 2004. Quantification of compartmented metabolic fluxes in developing soybean embryos by employing biosynthetically directed fractional (13)C labeling, two-dimensional [(13)C, (1)H] nuclear magnetic resonance, and comprehensive isotopomer balancing. Plant Physiology 136, 3043–3057.

Stelling, J., Klamt, S., Bettenbrock, K., Schuster, S., Gilles, E.D., 2002. Metabolic network structure determines key aspects of functionality and regulation. Nature 420, 190–193.

Stephanopoulos, G., Nielsen, J.B., Aristodou, A., 1998. Metabolic Engineering: Principles and Methodologies. Academic Press, San Diego.

Steuer, R., Gross, T., Selbig, J., Blasius, B., 2006. Structural kinetic modeling of metabolic networks. Proceedings of the National Academy of Sciences of the United States of America 103, 11868–11873.

Stitt, M., Quick, W.P., Schurr, U., Schulze, E.D., Rodermel, S.R., Bogorad, L., 1991. Decreased ribulose-1,5-bisphosphate carboxylase-oxygenase in transgenic tobacco transformed with 'antisense' rbcS. 2. Flux control coefficients for photosynthesis in varying light, CO_2, and air humidity. Planta 183, 555–566.

Sweetlove, L.J., Fernie, A.R., 2005. Regulation of metabolic networks: understanding metabolic complexity in the systems biology era. New Phytologist 168, 9–24.

Szyperski, T., 1998. ^{13}C NMR, MS and metabolic flux balancing in biotechnology research. Quarterly Reviews in Biophysics 31, 41–106.

Takahashi, K., Ishikawa, N., Sadamoto, Y., Sasamoto, H., Ohta, S., Shiozawa, A., Miyoshi, F., Naito, Y., Nakayama, Y., Tomita, M., 2003. E-CELL2: Multi-platform E-CELL simulation system. Bioinformatics 19, 1727–1729.

Teusink, B., Passarge, J., Reijenga, C.A., Esgalhado, E., van der Weijden, C.C., Schepper, M., Walsh, M.C., Bakker, B.M., van Dam, K., Westerhoff, H.V., Snoep, J.L., 2000. Can yeast glycolysis be understood in terms of in vitro kinetics of the constituent enzymes? Testing biochemistry. European Journal of Biochemistry 267, 5313–5329.

Thomas, S., Mooney, P.J.F., Burrell, M.M., Fell, D.A., 1997a. Finite change analysis of glycolytic intermediates in tuber tissue of lines of transgenic potato (*Solanum tuberosum*) overexpressing phosphofructokinase. Biochemical Journal 322, 111–117.

Thomas, S., Mooney, P.J.F., Burrell, M.M., Fell, D.A., 1997b. Metabolic control analysis of glycolysis in tuber tissue of potato (*Solanum tuberosum*): explanation of the low control coefficient of phosphofructokinase over respiratory flux. Biochemical Journal 322, 119–127.

Urbanczik, R., 2006. SNA – a toolbox for the stoichiometric analysis of metabolic networks. BMC Bioinformatics 13, 129.

van Winden, W., Heijnen, J.J., Verheijen, P.J.T., 2002. Cumulative bondomers: a new concept in flux analysis from ^{2}D, ^{13}C, ^{1}H-COSY NMR data. Biotechnology and Bioengineering 80, 731–745.

Varner, J., Ramkrishna, D., 1999. Mathematical models of metabolic pathways. Current Opinion in Biotechnology 10, 146–150.

von Kamp, A., Schuster, S., 2006. Metatool 5.0: fast and flexible elementary modes analysis. Bioinformatics 22, 1930–1931.

Wang, Z., Zhu, X.G., Chen, Y., Li, Y., Hou, J., Li, Y., Liu, L., 2006. Exploring photosynthesis evolution by comparative analysis of metabolic networks between chloroplasts and photosynthetic bacteria. BMC Genomics 7, 100.

Whittaker, A., Botha, F.C., 1997. Carbon partitioning during sucrose accumulation in sugarcane internodal tissue. Plant Physiology 115, 1651–1659.

Wiechert, W., 2001. ^{13}C metabolic flux analysis. Metabolic Engineering 3, 195–206.

Wiechert, W., Möllney, M., Isermann, N., Wurzel, M., de Graaf, A.A., 1999. Bidirectional reaction steps in metabolic networks: III. Explicit solution and analysis of isotopomer labeling systems. Biotechnology and Bioengineering 66, 69–85.

Wiechert, W., Möllney, M., Petersen, S., de Graaf, A.A., 2001. A universal framework for ^{13}C metabolic flux analysis. Metabolic Engineering 3, 265–283.

Wiechert, W., Nöh, K., 2005. From stationary to instationary metabolic flux analysis. Advances in Biochemical Engineering and Biotechnology 92, 145–172.

Xia, Y., Yu, H., Jansen, R., Seringhaus, M., Baxter, S., Greenbaum, D., Zhao, H., Gerstein, M., 2004. Analyzing cellular biochemistry in terms of molecular networks. Annual Review of Biochemistry 73, 1051–1087.

Ye, X., Al-Babili, S., Kloti, A., Zhang, J., Lucca, P., Beyer, P., Potrykus, I., 2000. Engineering the provitamin A (beta-carotene) biosynthetic pathway into (carotenoid-free) rice endosperm. Science 287, 303–305.

You, L., Hoonlor, A., Yin, J., 2003. Modeling biological systems using Dynetica–a simulator of dynamic networks. Bioinformatics 19, 435–436.

Yun, H., Lee, D.Y., Jeong, J., Lee, S., Lee, S.Y., 2005. MFAML: a standard data structure for representing and exchanging metabolic flux models. Bioinformatics 21, 3329–3330.

Zamboni, N., Fischer, E., Sauer, U., 2005. FiatFlux - a software for metabolic flux analysis from ^{13}C-glucose experiments. BMC Bioinformatics 25, 209.

Zimmer, W., Brüggemann, N., Emeis, S., Giersch, C., Lehning, A., Steinbrecher, R., Schnitzler, J.P., 2000. Process-based modelling of isoprene emission by oak leaves. Plant, Cell and Environment 23, 585–595.

Zupke, C., Stephanopoulos, G., 1994. Modeling of isotope distributions and intracellular fluxes in metabolic networks using atom mapping matrices. Biotechnology Progress 10, 489–498.

Rigoberto Rios-Estepa is a Fulbright scholar in the graduate program of Washington State University's Chemical Engineering and Bioengineering School. He received his Bachelor's and Master's degrees in Chemical Engineering from the National University of Colombia in Bogotá. After completing his thesis he worked as a Research Assistant at the Biotechnology Unit of the Colombian Petroleum Institute. He was appointed Assistant Professor at the Chemical Engineering Department of the University of Antioquia, Colombia and is currently on leave of absence to complete his graduate studies. His research interests focus around using mathematical modeling to enhance our understanding of the regulation of metabolic pathways.

Bernd Markus Lange is an Assistant Professor at the Institute of Biological Chemistry and the Center for Integrated Biotechnology at Washington State University. He received his Bachelor's and Master's degrees in Chemistry from the University of Bonn and his Doctoral degree in Botany from the University of Munich. Upon graduation, Dr. Lange held postdoctoral positions with Lutz Heide at the University of Tübingen and Rodney Croteau at Washington State University. Subsequently, he led research groups in the biotechnology industry (Novartis Agricultural Research Institute Inc., Torrey Mesa Research Institute of Syngenta and Diversa Inc.). His research interests center on using integrative approaches to characterize the regulation of biochemical pathways with particular emphasis on the crosstalk of pathways involved in isoprenoid biosynthesis.